Published in final edited form as:

Q J Nucl Med Mol Imaging. 2017 June ; 61(2): 181–204. doi:10.23736/S1824-4785.17.02969-7.

Radiolabeled inorganic nanoparticles for positron emission tomography imaging of cancer: an overview

Rubel CHAKRAVARTY[1,*], **Shreya GOEL**[2], **Ashutosh DASH**[1], and **Weibo CAI**[2,3,4,5]

[1]Radiopharmaceuticals Division, Bhabha Atomic Research Centre, Mumbai, India

[2]Materials Science Program, University of Wisconsin, Madison, WI, USA

[3]Department of Radiology, University of Wisconsin, Madison, WI, USA

[4]Department of Medical Physics, University of Wisconsin, Madison, WI, USA

[5]University of Wisconsin, Carbone Cancer Center, Madison, WI, USA

Abstract

Over the last few years, a plethora of radiolabeled inorganic nanoparticles have been developed and evaluated for their potential use as probes in positron emission tomography (PET) imaging of a wide variety of cancers. Inorganic nanoparticles represent an emerging paradigm in molecular imaging probe design, allowing the incorporation of various imaging modalities, targeting ligands, and therapeutic payloads into a single vector. A major challenge in this endeavor is to develop disease-specific nanoparticles with facile and robust radiolabeling strategies. Also, the radiolabeled nanoparticles should demonstrate adequate *in vitro* and *in vivo* stability, enhanced sensitivity for detection of disease at an early stage, optimized *in vivo* pharmacokinetics for reduced non-specific organ uptake, and improved targeting for achieving high efficacy. Owing to these challenges and other technological and regulatory issues, only a single radiolabeled nanoparticle formulation, namely “C-dots” (Cornell dots), has found its way into clinical trials thus far. This review describes the available options for radiolabeling of nanoparticles and summarizes the recent developments in PET imaging of cancer in preclinical and clinical settings using radiolabeled nanoparticles as probes. The key considerations toward clinical translation of these novel PET imaging probes are discussed, which will be beneficial for advancement of the field.

Keywords

Neoplasms; Molecular imaging; Nanoparticles; Positron-emission tomography; Theranostic nanomedicine

In the recent times, synthesis of functionalized nanoplatforms has demonstrated tremendous potential to greatly enhance the clinical armamentarium for cancer theranostics.[1, 2]

[*]Corresponding author: Rubel Chakravarty, Radiopharmaceuticals Division, Bhabha Atomic Research Centre, Trombay, Mumbay 400085, India. rubelc@barc.gov.in.

Conflicts of interest.—The authors certify that there is no conflict of interest with any financial organization regarding the material discussed in the manuscript.

Extensive research efforts at the interface between materials science and biomedicine have resulted in exceptional accomplishments toward syntheses of various types of nanoplatforms that can directly be used for biomedical research.[1, 2] Today, increasing numbers of nanoparticle-based diagnostic or therapeutic agents are either being commercialized or have reached the clinical stage, thereby, achieving important milestones in “bench-to-bedside” translation of nanotechnology.[3–5] The overwhelming enthusiasm of the scientific community in this field can be understood from the fact that >133,600 articles on “nanoparticles” were reported in PubMed as of December 2016, more than half of which were published after the year 2010.

Nanoparticles exhibit unique size-dependent physical and chemical properties, which if properly harnessed can address unsolved challenges in clinical oncology.[1, 2] Particularly, they possess large functional surface area, easily controllable surface chemistry that facilitates surface functionalization to achieve tailored characteristics for effective use in personalized cancer management.[1, 2] In the endeavor toward translating this promise into clinical reality, visualization of the distribution of nanoparticle-based carriers in the body following systemic administration through any route is of paramount importance. Presently, the most prudent approach that provides quantitative information about the whole body biodistribution is by incorporating suitable radioisotopes in the nanoparticles — a process known as “radiolabeling”.[2, 6, 7] After administration of the radiolabeled nanoparticles in living subjects, their *in vivo* biodistribution can be non-invasively monitored by molecular imaging techniques such as single photon emission computed tomography (SPECT),[8] PET,[9] Cerenkov luminescence (CL),[10] Cerenkov resonance energy transfer (CRET),[11] etc., that are now been widely explored for cancer imaging in preclinical and/or clinical settings.

The advantages of using radiolabeled nanoparticles for molecular imaging applications are many-fold.[7] Radiolabeled nanoparticles can act as signal amplifiers, leading toward enhanced contrast indices and increased sensitivity compared to conventional radiotracers. Owing to the large surface area of nanoparticles, they can be conjugated with different targeting ligands for targeted detection of various types of cancers. Also, nanoparticles offer the scope of multimodality imaging which provides synergistic advantages over any one single molecular imaging modality alone. The third advantage lies in the ability of nanoparticles to combine both diagnostic and therapeutic capabilities onto the same nanoplatform, giving rise to the emerging concept of “image-guided drug delivery”.[8, 9] Additionally, different therapeutic agents (chemotherapeutic drugs as well as suitable therapeutic radioisotopes) can be incorporated in the same nanoplatform which might be a viable option toward multimodality targeted therapy for improved cancer management.

Generally, nanoparticles used for cancer research can be broadly categorized into four groups: 1) inorganic nanoparticles such as quantum dots, metal nanoparticles, iron oxide nanoparticles, silica nanoparticles, metal sulfide nanoparticles and upconversion nanophosphors; 2) polymer nanoparticles such as core-shell dendrimers, and amphiphilic nanoparticles; 3) lipid nanoparticles such as liposomes and solid lipid nanoparticles; and 4) carbon based nanoparticles, such as, carbon nanotubes, graphene oxide and nanodiamonds. In this concise review, we have focused on the recent developments in utilization of radiolabeled inorganic nanoplatforms for PET imaging of various types of cancers in

preclinical and clinical settings. The different methods for radiolabeling of nanoparticles have been described along with their pros and cons. The advantages of using radiolabeled nanoparticles have been highlighted and the barriers toward their successful clinical translation are discussed to provide an overview of the future challenges and opportunities. Because of the vast amount of work that has been carried out in this field, we restrict the discussion to recent and illustrative examples only and apologize for possible oversights of important contributions.

PET imaging using radiolabeled nanoparticles

Molecular imaging of cancer using radiolabeled nanoparticles may be used for early detection, characterization, and staging of the disease and also for monitoring the efficacy of therapeutic drugs.[2, 7] Among various imaging modalities used, PET imaging technology provides highly sensitive and quantitative information and is expected to play an increasingly important role in earlier disease detection and improved therapeutic decision making.[12, 13] In PET, the radioisotope incorporated in the nanoparticle decays resulting in the emission of positrons which interact with nearby electrons after travelling a short distance (~1 mm) within the body.[13] Each positron-electron annihilation process produces two 511-keV γ-photons in opposite directions, and these two gamma photons may be detected by the detectors surrounding the subject to precisely locate the source of the decay event. Subsequently, the “coincidence events” data can be processed by computers to reconstruct the spatial distribution of the radiolabeled nanoparticles and the PET images thus generated can reflect the concentration and *in vivo* distribution of the radiotracer administered.

For successful PET imaging using radiolabeled nanoparticles, there are four important parameters which need to be carefully considered: 1) choice of the radioisotope; 2) choice of a suitable nanoplatform; 3) radiolabeling method; and 4) stability of the radiolabeled agent. These aspects are briefly discussed below.

Choice of the radioisotope

The choice of a suitable radioisotope for radiolabeling with nanoparticles is based on the following criteria: 1) nuclear decay characteristics of the radioisotope; 2) ease of production and convenient availability of the radioisotope; and 3) reliability of the radiolabeling strategy.[2, 13] Ideally, radioisotopes with low positron energy and high β^+ branching ratio are favorable for PET imaging. Generally, in case of radioisotopes with high positron energy, the β^+ particles travel a longer distance before positron annihilation takes place which results in loss of spatial resolution. For radioisotopes with low β^+ branching ratio, long scan times would be required and PET images obtained would often be noisy. The emission of high energy γ-photons from the positron-emitting radioisotope (*e.g.* ^{86}Y which emits 1.7 MeV, 0.95 MeV, 0.84 MeV, etc. γ-photons) is another undesirable phenomenon as it would not only affect the PET image quality but also give unnecessary dose to normal organs. Another parameter of concern is the decay half-life of the radioisotope. Generally, the very short-lived radioisotopes (*e.g.* ^{11}C; $t_{½}$=20 min, ^{15}O; $t_{½}$=2 min) are not suitable as there would be considerable decay loss during the radiolabeling procedure. Also, the utility of such short-

lived radioisotopes is restricted to institutions having on-site cyclotron facility and transportation to distant user sites is not possible. For molecular imaging of cancer using PET, the half-life of the radioisotopes should match the biological half-life of the functionalized nanoparticles in order to allow them to reach the target of interest. Further, it is important that the decay time is as short as possible in order to avoid unnecessary radiation exposure. However, for nanoparticles with prolonged circulation *in vivo*, relatively longer lived radioisotopes would be required for radiolabeling in order to monitor the clearance profile. From the perspective of future clinical translation, the production route should be simple and it should be possible to obtain the radioisotope in adequate quantity for formulation of clinically relevant doses of the radiolabeled agent for PET imaging in human subjects. Last, but not the least, a suitable radiolabeling strategy must be chosen based on the chemistry of the radioisotope and the specific application which is intended to be studied. The nuclear characteristics of commonly used positron emitting radioisotopes are summarized in Table I and the production and decay scheme are illustrated in Figure 1.

Choice of the suitable nanoplatform

The choice of the suitable nanoplatform for radiolabeling is based on the specific application for which it is intended. The important factors that guides the choice of the nanoplatform include, chemical composition, inherent functionality and surface characteristics, ease of surface modifications, hydrodynamic diameter, ability to add diagnostic and therapeutic agents, amenability for conjugation with ligands for active targeting, colloidal stability in physiological medium, etc. Sometimes, for effective cancer management, it is desirable to utilize the radiolabeled nanoparticles for multimodality imaging. [6] In such cases, the inherent properties of nanoparticles may be suitably controlled so that the nanoparticle itself becomes an imaging agent, in addition to its PET imaging characteristics conferred by the radioisotope attached.[6] Some typical examples of using the inherent properties of inorganic nanoparticles for imaging include fluorescent emissions from quantum dots,[14] use of superparamagnetic iron oxide particles (SPIONs) as magnetic resonance imaging (MRI) contrast agents, etc.[15, 16] Alternatively, a suitable dye could be incorporated in the functionalized nanoparticles (such as silica nanoparticles) for PET/optical dual modality imaging.[17] When the nanoparticle is intended to be used for PET image guided drug delivery, it is prudent to choose a nanoplatform that ensures precise targeting, accurate dose delivery, and minimal toxicity in order to achieve maximal therapeutic efficacy.[9]

From the perspective of future clinical translation of the radiolabeled inorganic nanoparticles, it might be advantageous to choose biocompatible nanoparticles (such as silica, iron oxide or gold nanoparticles),[5] which have already been used in clinical context for other applications as their safety, efficacy and reliability have been established to a considerable extent. Biodegradability and renal clearance behavior of the administered nanoparticles are other important criteria that are being seriously considered in the recent times from the view point of clinical translation.[18]

Radiolabeling methods

Ideally, a radiolabeling method should be robust, rapid, safe, should introduce minimal changes to the original characteristics of the nanoparticles and be reasonably efficient. It is also of paramount importance to ensure that the entire radiolabeling process is executed while strictly adhering to the "as low as reasonably achievable (ALARA)" guidelines for radioactivity handling processes. High reaction temperature, prolonged reaction time, and multi-step purification strategies, which pose a threat for both the properties of nanoparticles and the health of operators, should be avoided. There are four major radiolabeling strategies: 1) complexation reaction of radiometal ions with chelators via coordination chemistry; 2) direct bombardment of nanoparticles via hadronic projectiles; 3) synthesis of intrinsically radiolabeled nanoparticles using a mixture of radioactive and non-radioactive precursors; 4) chelator-free post-synthetic radiolabeling (Figure 2). Each of these radiolabeling methods has its own advantages and limitations, and the choice of a particular radiolabeling method should be based on the specific radioisotope, research purpose, and feasibility.

The most widely used radiolabeling method till today is by coordination of the radiometal to the nanoparticle via a chelator. In this perspective, a wide range of radiometal ions with different nuclear characteristics are available and can be used depending on the type of applications (Table I, Figure 1).[19] A wide variety of chelators such as 1,4,7-triazacyclononane-1,4,7-triacetic acid (NOTA), 1,4,7,10-tetraazacyclododecane-1,4,7,10-tetraacetic acid (DOTA), desferrioxamine (Df), diethylene triamine pentaacetic acid (DTPA), etc., are available for this purpose and the choice of a particular chelator is based on the coordination chemistry of the radiometal ion used for radiolabeling.[20, 21] This approach is generally applicable to different nanomaterials with the help of well-designed surface chemistry. Though, this strategy is relatively easy to operate, it requires significant structural/surface modifications which can often affect the pharmacokinetics of nanoparticles leading to suboptimal targeting and *in vivo* distribution. The other limitations include, potential dissociation of the radiometal containing chelator in the presence of high protein concentration in blood stream, or transchelation of the radiometal from the chelator-complex which might lead to erroneous interpretation of the PET imaging results.

In view of the limitations of the conventional chelator based radiolabeling methods, development of new radiolabeling approaches was deemed essential to advance nanomedicine. The unique characteristics of inorganic nanoparticles allow radiolabeling without using the chelators. One option is by direct irradiation of as-synthesized nanoparticles in nuclear reactors or cyclotrons to generate radiolabeled nanoparticles. For example, direct proton irradiation has been applied to ^{18}O enriched Al_2O_3 nanoparticles to produce to produce ^{18}F-labeled Al_2O_3 nanoparticles via the ^{18}O (p, n) ^{18}F nuclear reaction.[22] In this case, the radioisotope was incorporated inside the nanoparticles and the PET signal was believed to actually reflect the distribution of nanoparticles without leaking. However, this strategy is greatly limited by the access to the nuclear reactors or cyclotrons for irradiation of the nanoparticles. Moreover, preparation of suitable targets for irradiation without compromising on the properties of the nanoparticles would pose complex challenges. More importantly, bombardment of the nanoparticles with hadronic projectiles such as protons or neutrons might affect the properties of the nanoparticles, especially when

the nanoparticle surface is conjugated with biologically active molecules. Therefore, the practicality of this method is limited.

Another method to incorporate radioisotopes inside nanoparticles is to use radioactive precursors to synthesize intrinsically radiolabeled nanoparticles.[23] Depending on the specific activity of the radioactive precursors (which in turn depends on the nuclear reaction by which the radioisotope is produced), they may be mixed with non-radioactive analogs. In case of such intrinsically radiolabeled nanoparticles, the radioisotopes are built inside the crystal lattice of the nanocrystals, resulting in high radiochemical stability.[23] One of the most widely studied intrinsically radiolabeled inorganic nanoparticles for PET imaging is ^{64}CuS nanoparticles, generally synthesized by metathesis reaction of $^{64}CuCl_2$, $CuCl_2$, and Na_2S at 95 °C for 1 h.[24] It is pertinent to point here that this strategy involves risks of radioactive contamination and radiation exposure to the working personnel. Therefore, it is essential to perform the entire process in a shielded facility, preferably, in a hot-cell equipped with remotely operable gadgets to minimize the radiation hazards.

Over the last few years, post-synthesis radiolabeling of nanoparticle based on chelator-free approach is gaining popularity.[23] This approach takes advantage of the specific physical or chemical interaction between certain radionuclide ions and nanoparticles to integrate the radioisotopes into as-prepared nanoparticles with negligible effect on their intrinsic characteristics. The chelator-free uptake of radioisotopes by the nanoparticles is generally based on 1) specific trapping of certain radionuclide ions into the nanoparticles by formation of some sort of bonding and 2) ion-exchange mechanisms. Specific trapping of radionuclide ions has been widely used and has demonstrated to be highly promising for a number of radioisotopes (such as ^{64}Cu,[25] ^{89}Zr,[26] ^{72}As,[27] and ^{69}Ge,[28] etc.) and nanoparticles. Ion exchange based approaches have also been utilized to radiolabel lanthanide- doped upconversion nanoparticles with ^{18}F [29] and ^{64}Cu [30] for PET imaging. The chelator-free post-synthetic radiolabeling strategy is generally fast and specific and can achieve high radiolabeling yield under mild reaction conditions. However, this strategy is yet to be applied for a wide variety of radioisotopes and nanoparticles.

Stability of radiolabeled nanoparticles

Generally, two types of stabilities are important for radiolabeled nanoparticles: 1) colloidal stability and 2) radiochemical stability.[13] Excellent colloidal stability is an essential criterion for using nanoplatforms for molecular imaging applications. The colloidal stability of nanoparticles dispersed in a particular medium can be assessed by measurement of the hydrodynamic diameter by dynamic light scattering (DLS) technique [31] or by monitoring magnetic T_2 relaxation time [32] over a prolonged period of time. In addition to colloidal stability, radiochemical stability is also crucial for radiolabeled nanoparticles. Dissociation of radioisotopes from the nanoparticles would result in uptake of radioactivity in non-targeted organs and PET imaging will not be able to truly reflect the distribution of radiolabeled nanoparticles when administered *in vivo*.

Taking into consideration the complexities of different nanoparticles which include size, shape, surface charge and multiple attachments, there is no universal method for evaluating the radiochemical stability of nanoparticles. Generally, the radiolabeled nanoparticles are

incubated under physiological conditions (PBS or mouse serum with or without challenging agents such ethylenediaminetetraacetic acid [EDTA]) at 37 °C over a prolonged period of time and the level of detached radionuclide is estimated by size exclusion chromatography using PD-10 columns or centrifugal filtration.[32] The radiochemical stability of radiolabeled nanoparticles can also be evaluated by PET imaging studies in mice models. If the radiolabeled nanoparticles are not radiochemically stable after *in vivo* administration, the detached radioisotopes would rapidly be excreted from the mice via the renal route resulting in strong radioactivity signal in the bladder. In some cases, the detached radionuclides might demonstrate persistent uptake in certain organs (*e.g.* bone uptake for ^{89}Zr), which can easily be differentiated from the radiolabeled nanoparticles by PET imaging.

Targeting of radiolabeled inorganic nanoparticles to the tumor tissue

The delivery of the radiolabeled nanoparticles to the target tissue can be achieved primarily in two ways — passive and active targeting (Figure 3).[33] Passive targeting takes advantage of the permeability of tumor tissue. [33] Due to rapid vascularization to serve fast-growing cancerous tissues, the capillary endothelium in cancerous tissue is more disordered and thus more permeable towards nanoplatforms than the capillary endothelium in normal tissues. If the radiolabeled nanoparticles can stay in blood circulation for a reasonably long time, there will be enrichment of nanoplatforms into the tumor tissues. Furthermore, since the lymphatic system is not developed in tumor tissue, the nanoparticles tend to stay inside the interstitial space in tumor tissues. This overall phenomenon of accumulation of nanoplatforms in tumor tissues is known as the enhanced permeability and retention (EPR) effect.[33, 34]

The EPR phenomenon is dependent on several factors such as particle size, particle surface charge and hydrophobicity, immunogenicity, tumor characteristics, etc., which results in many challenges in the optimization of passive targeting.[33] Further, specificity towards the tumor would be low in passive targeting and therefore therapeutic concentrations of the chemotherapeutic drug can be suboptimal at the tumor site resulting in poor therapeutic efficacy.[33] To overcome these limitations, active targeting would be a more viable approach which can be achieved by conjugating the functionalized nanoplatform to a suitable targeting ligand such as aptamers, peptides or proteins, thereby allowing preferential accumulation of the drug in the tumor tissue.[33] The best results would be expected by combining the effects of both passive as well as active targeting to achieve maximal therapeutic efficacy.[33]

The introduction of biocompatible hydrophilic polymer chains, such as polyethylene glycol (PEG), creates a hydrated brush-like coating on the nanoparticle surface thereby enhancing nanoparticle solubility, prolongs blood circulation times, and delays clearance by mononuclear phagocyte system (MPS).[35] It has been demonstrated that PEG-coated nanoplatforms have circulation times several orders of magnitude longer than uncoated nanoplatforms and demonstrate significantly higher tumor uptake.[35]

Preclinical studies with radiolabeled inorganic nanoparticles

Several inorganic nanoplatforms such as quantum dots, metallic nanoparticles, oxide nanoparticles, upconversion nanoparticles, CuS nanoparticles, etc., have been radiolabeled with different positron emitter radionuclides and used as probes for PET imaging of cancer in preclinical settings. Most of these studies are summarized in Table II [36–115] and described in the following text.

Radiolabeled quantum dots

Over the past decade, functionalized quantum dots have been widely explored for *in vivo* biomedical imaging due to their favorable properties, such as, high quantum yield, resistance to photobleaching, narrow emission peak, and tunable emission wavelength.[14, 36–38] Radiolabeling of quantum dots with positron emitting radioisotopes confers PET functionality for use as a probe for dual modality PET/optical imaging. In a preliminary study, Schipper *et al.* evaluated the comparative biodistribution of PEGylated and non-PEGylated CdSe quantum dots of two different sizes (12 nm and 21 nm diameter) in mice.[39] The quantum dots were conjugated with DOTA chelators, radiolabeled with ^{64}Cu, and administered in normal mice. *In vivo* PET imaging studies revealed that size of the quantum dots had no influence on biodistribution and rapid uptake of activity was observed in the liver (27.4–38.9 %ID/g) and spleen (8.0–12.4 %ID/g). No evidence of clearance of the radiolabeled quantum dots from these organs was observed, suggesting that further modification of the quantum dots would be required for use as molecular imaging probe. In an improved study, the same group later demonstrated that PEGylation and peptide (QDC) coating of quantum dots significantly reduced their uptake in liver and spleen and accelerated clearance from these organs than observed in the previous study.[40] Further, it was seen that the smaller sized quantum dots (2-nm diameter) cleared by both renal as well as hepatobiliary route. In another similar study, Tu *et al.* synthesized dextran coated silicon quantum dot conjugated with DO3A (1,4,7,10-tetraazacyclododecane-1,4,7-triacetic acid) chelator for ^{64}Cu labeling.[41] The radiolabeled quantum dots showed high radiochemical stability. *In vivo* PET imaging studies showed that the radiolabeled agent cleared by both renal as well as hepatobiliary route. The results of these studies showed that the modified quantum dots are suitable for use as molecular imaging probes.

For the first time, Cai *et al.* reported the utility of radiolabeled quantum dots for PET/near infrared fluorescence imaging of tumor vasculature.[42] For this purpose, an amine functionalized quantum dot (QD705; emission maximum, 705 nm; Invitrogen) was conjugated with RGD peptide for integrin $\alpha_v\beta_3$ targeting and DOTA chelator for ^{64}Cu labeling. The radiolabeled quantum dots were administered in mice bearing human glioblastoma xenograft (U87MG) and PET/near infrared fluorescence imaging, tissue homogenate fluorescence measurement, and immunofluorescence staining were performed to measure the probe uptake in tumor and major organs. The tumor uptake of the radiolabeled quantum dots peaked at 15 h postinjection (~4 %ID/g) with good tumor-to-background contrast. Further, excellent linear correlation was observed between the results obtained from *in vivo* PET imaging, *ex vivo* near infrared fluorescence imaging and tissue homogenate fluorescence. The histological studies revealed that the RGD conjugated

quantum dots primarily targets the tumor vasculature through interaction of RGD moiety with integrin $\alpha_v\beta_3$, with little extravasations. In a similar study, Hu et al demonstrated the utility of quantum dots modified with β-Glu-RGD-BBN (RGD=arginine-glycine-aspartate acid, and BBN=bombesin) peptides and radiolabeled with ^{18}F *via* the 4-nitrophenyl-2-^{18}F-fluoropropionate prosthetic group for dual modality PET/near infrared fluorescence imaging in prostate (PC-3) tumor bearing mice.[43] The major advantage of these studies was that it could overcome the tissue penetration limitation of near infrared fluorescence imaging, thereby allowing quantitative *in vivo*-targeted dual modality (PET/near infrared fluorescence) imaging in deep tissues.

Over the last few years, there has been tremendous interest in development of self-illuminating quantum dots, with no need for an external light source, based on CRET.[44] Cerenkov luminescence is produced when high energy charged particles (β^+, β^- or α particles) travel through a dielectric medium (*e.g.* water), with a velocity that exceeds the speed of light in that medium. Generally, Cerenkov luminescence spectra are continuous and more intense at higher frequencies (ultraviolet/blue). Owing to the fact that ultraviolet/blue wavelengths are highly attenuated by tissues, Cerenkov luminescence itself is not sufficient for *in vivo* imaging. [45] In the quantum dot-CRET system, the Cerenkov luminescence energy is transferred to the quantum dots in close proximity. This phenomenon can help convert the blue-weighted Cerenkov luminescence to longer quantum dots emission wavelengths which allows for *in vivo* optical imaging in animal models.[46] Sun *et al.* reported the synthesis of self-illuminating quantum dots which exhibit efficient CRET process, by controlled doping of ^{64}Cu into CdSe/ZnS core/shell quantum dots via a cation-exchange reaction.[30] The radiolabeled quantum dots demonstrated excellent radiochemical stability and were administered in mice bearing glioblastoma (U87MG) xenografts. *In vivo* PET imaging showed high tumor uptake (12.7 %ID/g) at 17 h post-injection (p.i.) with good tumor-to-background contrast (Figure 4A). Also, the feasibility for *in vivo* luminescence (CRET) imaging of tumor in the absence of excitation light was demonstrated (Figure 4B). In another interesting study, Guo *et al.* synthesized intrinsically radioactive [^{64}Cu] CuInS/ZnS quantum dots by directly incorporating ^{64}Cu into CuInS/ZnS nanostructure and similar results were obtained.[47] These studies amply demonstrated that the synergistic advantages provided by CRET-quantum dot systems would find widespread utility toward multimodality cancer imaging.

Radiolabeled metal nanoparticles

Among various metallic nanoparticles reported to date, radiolabeled gold nanoparticles are most predominantly studied for use in molecular imaging due to their unique size-dependent physicochemical and optical properties, biocompatibility, ease of characterization, and rich surface chemistry.[48] For the first time, Xie et al reported the synthesis of gold nanoshells which were PEG modified and conjugated with DOTA-based chelator for radiolabeling with ^{64}Cu.[49] The radiolabeled nanoparticles were administered in nude rats bearing human head and neck squamous cell carcinoma xenograft. *In vivo* PET imaging and biodistribution studies showed low tumor uptake (<1 %ID/g), undermining the utility of this radiolabeled agent for cancer imaging. In another study, Guerrero *et al.* reported the radiolabeling of Au nanoparticles with ^{18}F for use as a PET radiotracer.[50] In this study, N-succinimidyl-4-[^{18}F]-

fluorobenzoate was covalently linked to Au nanoparticles conjugated with amphipathic peptide, CLPFFD. *In vivo* PET imaging in rats after administration of the radiolabeled nanoparticles showed that they cleared through both hepatobiliary as well as renal route. In a similar study, Zhu *et al.* reported the synthesis of water-soluble maleimide-terminated PEGylated Au nanoparticles (3 nm diameter) which could be radiolabeled by reaction with silicon-fluorine prosthetic group, [^{18}F]SiFA -SH and used for PET imaging in healthy rats.[51] In another study, Wang *et al.* reported the synthesis of Au nanocages of two different sizes (55 nm and 30 nm in edge length) and used them for radiolabeling with ^{64}Cu.[52] *In vivo* PET imaging studies in normal C57BL/6 mice showed that the 30 nm nanocages had a greatly improved biodistribution profile than 55 nm nanocages, together with higher blood retention and lower uptake in liver and spleen. Additionally, in mice bearing murine EMT-6 breast tumor, the 30 nm cages also showed a significantly higher level of tumor uptake (~ 8 %ID/g versus 2 %ID/g at 4 h p.i.) and a greater tumor-to-muscle ratio than the 50 nm cages. These results of these preliminary studies demonstrated the utility of radiolabeled Au nanoparticles for PET imaging.

The utility of Au nanoparticles for PET image guided drug delivery was first reported by Xiao *et al.*[53] The authors synthesized Au nanorods conjugated with doxorubicin and cRGD peptide and radiolabeled with ^{64}Cu. *In vivo* PET imaging studies in mice bearing U87MG tumors after administration of radiolabeled Au nanoparticles, showed high tumor uptake (6.4±1.2 %ID/g within 1 h p.i.) with good tumor-to-background contrast. This approach might find utility in combined cancer therapy (chemotherapy and photothermal therapy) and multimodality imaging (PET, CT, etc.). Later, Tian *et al.* reported the synthesis of hollow gold nanospheres (40 nm in diameter) which could be conjugated with cRGD peptide for integrin $\alpha_v\beta_3$ targeting and DOTA chelator for ^{64}Cu labeling.[54] The radiolabeled nanoparticles were used for PET/CT imaging in a rabbit VX2 liver cancer model. The authors demonstrated that liver tumor targeting of radiolabeled Au nanospheres could be improved by using intra-arterial administration and by mixing the nanoparticles with iodized oil such as lipiodol. In another interesting study, Cheng *et al.* reported the synthesis of anisotropic, branched, gold nanoarchitectures (Au-tripods), conjugated with cRGD peptide and NOTA chelator for ^{64}Cu labeling.[55] The radiolabeled nanoplatform could be used as a dual modality (photoacoustic imaging/PET) imaging agent for tumor angiogenesis in U87MG tumor bearing mice. *In vivo* PET imaging data revealed showed high tumor uptake (~7.9 %ID/g at 24 h p.i.) of the radiolabeled nanoplatform. The photoacoustic imaging results correlated well with the corresponding PET images, further demonstrating the suitability of Au-tripods for multimodality molecular imaging.

With an objective to evaluate blood-brain barrier (BBB) permeability, Frigell *et al.* developed water soluble glucose coated Au nanoparticles (2 nm size) attached with different BBB-permeable neuropeptides and NOTA chelator.[56] The nanoconjugates were radiolabeled with ^{68}Ga and used for PET imaging studies after intravenous injection in normal rats. Depending on the nature of targeting ligands (neuropeptides) attached to Au nanoparticles, different biodistribution profiles were observed. For Leu-enkephalin peptide, targeted Au nanoparticles demonstrated significantly improved brain accumulation (0.020±0.0050 %ID/g) compared to non-targeted Au nanoparticles (0.0073±0.0024 %ID/g). Even though brain accumulation reported is low and results presented are preliminary, this

study suggests that further manipulation of the targeting molecules conjugated to Au nanoparticles might result in more favorable properties to cross the BBB for enhanced brain uptake.

Adopting an interesting approach, Lee *et al.* synthesized Au nanoparticles of 20-nm core size, which were then modified with thiolated oligonucleotides consisting of ten adenine bases.[57] This surface modification of Au nanoparticles allowed for radiolabeling with ^{124}I. The radiolabeled nanoparticles demonstrated high *in vitro* and *in vivo* stability and were used for detection of sentinel lymph nodes by combined PET and Cerenkov luminescence imaging. Such radiolabeled Au nanoparticle based lymphatic tracers might be useful for pre- and intra-operative surgical guidance. In a recent study, Chen *et al.* reported the synthesis of ultrasmall sized (hydrodynamic diameter=2.5 nm), renal clearable Au nanoparticles conjugated with NOTA chelator for ^{64}Cu labeling.[58] Dynamic PET imaging in mice showed rapid renal clearance of the radiolabeled Au nanoparticles and its elimination half-life was calculated to be <6 minutes. This study might be useful in understanding the renal clearance mechanisms and diagnosis of the kidney diseases in future.

Nanoclusters are an emerging class of nanomaterials that hold tremendous promise in molecular imaging applications due to their unique sizes and related optical properties.[59] Hu *et al.* reported the synthesis intrinsically ^{64}Cu-labeled Au nanocluster (~2.5 nm diameter) using bovine serum albumin (BSA) as the template.[60] The nanoclusters were synthesized with excellent stability and water solubility *in vitro*, and non-cytotoxicity and appreciable biocompatibility *in vivo*. BSA acts both as a reducing as well as stabilizing agent in the synthesis reaction. In the radiolabeled nanocluster, ^{64}Cu plays dual roles as: 1) a radionuclide for PET imaging; and 2) energy donor to excite Au nanocluster for self-illuminating near infrared fluorescence imaging based on CRET. The radiolabeled nanocluster exhibited efficient dual modality (CRET/PET) imaging both *in vitro* and *in vivo* (Figure 5).[60] When the radiolabeled nanocluster was administered in U87MG tumor bearing mice, high tumor uptake (14.9 %ID/g at 18 h p.i.) was observed *by in vivo* PET imaging. Also, satisfactory self-illuminating near infrared images of the tumor were generated in the absence of external excitation. Adopting a similar approach, synthesis of intrinsically radiolabeled ^{64}Cu [Cu] nanoclusters were reported using BSA as a scaffold for PET imaging in an orthotropic lung tumors in mice model.[61] Also, synthesis of similar ^{64}Cu-labeled Au nanoclusters were reported using other methods and used for PET imaging of cancer in preclinical settings.[62, 63]

In a recent study, Frellsen *et al.* reported a chelator free approach for radiolabeling Au nanoparticles with ^{64}Cu.[64] Citrate capped Au nanoparticles were synthesized by conventional method and incubated with $^{64}Cu^{2+}$ ions, followed by trapping of the radionuclide by grafting on a second layer of gold. The radiolabeled nanoparticles demonstrated excellent *in vitro* and *in vivo* stability. The ^{64}Cu-labeled Au nanoparticles were subsequently modified with different surface coatings and administered in mice for PET imaging studies. Highest tumor uptake (3.9 %ID/g) resulted from PEG coating, while faster removal from the bloodstream was observed with both a Tween 20-stabilized coating and a zwitterionic coating based on a mixture of sulfonic acids and quaternary amines.

Taken together, all these studies amply demonstrated the potential of intrinsically radiolabeled metal nanoclusters as novel imaging contrast agents.

Radiolabeled silica nanoparticles

Over the last few years, there has been a rapid development in the design and synthesis of various types of silica based nanoplatforms for potential use in cancer theranostics because of the non-toxic nature and facile chemistry of such nanoplatforms facilitating surface modifications.[65] In an initial study, Huang *et al.* reported the synthesis of mesoporous silica nanoparticles for use in multimodality imaging.[66] A near infrared dye (ZW800) was incorporated in the nanoparticles during the synthesis process and the nanoparticles were subsequently labeled with T_1 contrast agent Gd^{3+} and radionuclide ^{64}Cu through chelation reactions. *In vitro* studies confirmed the stability and intracellular retention times of the synthesized nanoplatform. The radiolabeled nanoparticles were successfully used for multimodality (PET/optical/MR) imaging of sentinel lymph nodes in mice. Subsequently, in a more advanced study, Chen *et al.* developed surface functionalized mesoporous silica nanoparticles (~80-nm size) for *in vivo* tumor vasculature targeted imaging and enhanced drug delivery. [67] The nanoparticles were conjugated to TRC105 (a human/murine chimeric IgG_1 monoclonal antibody, which binds to CD105/endoglin receptor) and NOTA chelator through PEG linkers. The nanoconjugate was subsequently radiolabeled with ^{64}Cu and administered in mice bearing murine breast (4T1) carcinoma. *In vivo* PET imaging studies showed significant tumor uptake (~6 %ID/g) within 5 h p.i. and the specificity of the radiotracer was demonstrated by non-targeted and blocking studies (Figure 6).[67] The authors also successfully demonstrated enhanced tumor-targeted delivery of doxorubicin (DOX) after intravenous injection of DOX loaded nanoconjugate in 4T1 tumor bearing mice. Subsequently, the same group of authors utilized mesoporous silica nanoparticles for multimodality imaging and tumor targeted drug delivery after conjugation of the nanoparticles with Fab fragment of TRC105[68] and anti-vascular endothelial growth factor receptor (VEG-FR) ligand, $VEGF_{121}$.[69] With an objective to achieve enhanced tumor-targeted drug-delivery along with PET imaging, the authors further synthesized hollow mesoporous silica nanoparticles conjugated with TRC105[70] and RGD peptide,[71] loaded with anticancer drugs and radiolabeled with ^{64}Cu. The drug loading capacity in hollow mesoporous silica nanoparticles was 3–15 times higher than that of mesoporous silica nanoparticles. All these studies hold great promise for future image-guided drug delivery applications using mesoporous silica-based nanoplatforms.

In an interesting report, Lee *et al.* demonstrated pretargeting approach using mesoporous silica nanoparticles for PET imaging in U87MG tumor bearing mice.[72] This approach is based on the highly bioorthogonal and rapid strain-promoted alkyne azide cycloaddition-based conjugation reaction using ^{18}F. For this study, aza-diben-zocyclooctynes functionalized and PEGylated mesoporous silica nanoparticles were synthesized, which could accumulate in the tumor by EPR effect when intravenously administered in mice. The ^{18}F-labeled synthon when administered could rapidly react with the nanoplatform *in vivo* and PET imaging studies showed significant tumor uptake (~1.5 %ID/g) with excellent tumor-to-background contrast. This pre-targeting approach is particularly important while using short lived radioisotopes for radiolabeling nanoparticles, which generally require a

long circulation time in the body to demonstrate decent tumor uptake by EPR effect. Also, this strategy reduces the radiotracer uptake in healthy organs, thereby improving the image contrast.

In a different study, Miller *et al.* developed a strategy for radiolabeling mesoporous silica nanoparticles with ^{89}Zr using Df-based chelator.[73] The radiolabeled agent demonstrated good *in vitro* and *in vivo* stability and could be used as a PET imaging probe in mouse model. The chelator-free approach for radiolabelling nanoparticles is becoming increasingly popular in the present times.[23] Chen *et al.* developed chelator-free method for ^{89}Zr labeling of mesoporous silica nanoparticles with high *in vivo* stability over a prolonged period of time (>20 days).[74] The radiolabeling and *in vivo* stability of the nanoplatform were found to be dependent on the concentration and location of deprotonated silanol groups in the nanoparticles. In similar studies, Shaffer *et al.* developed chelator-free methods for radiolabeling ^{68}Ga [26 and] ^{64}Cu [75] with mesoporous silica nanoparticles. These radiolabeling studies might be useful in understanding the short and long term fate of mesoporous silica nanoparticles when administered *in vivo* for PET image guided drug delivery applications.

Recently, Goel *et al.* synthesized dendritic, biodegradable mesoporous silica nanoparticles with potential to carry multiple cargos and subsequently self-destruct after release of payloads.[76] The nanoparticles were PEGylated, conjugated with TRC105 and radiolabeled with ^{89}Zr via the chelator-free approach. *In vivo* PET imaging in 4T1 tumor bearing mice showed rapid tumor uptake which peaked to ~11.5 %ID/g at 4 h p.i., remaining constant afterwards up to 48 h p.i. This approach of using radiolabeled biodegradable nanoplatforms can possibly pave the way for future personalized nanotheranostics.

Radiolabeled iron oxide nanoparticles

Iron oxide nanoparticles are a well-established class of nanoplatforms that has been actively investigated as MRI contrast agents in clinical trials.[77–79] They have also been employed as dual modality PET/MR imaging probes after being radiolabeled with suitable positron emitters. In 2008, Lee *et al.* reported the synthesis of polyaspartic acid-coated iron oxide nanoparticles (core size 5 nm, hydrodynamic diameter 45 nm) which were then used for PET/MR imaging.[80] As-synthesized nanoparticles were PEGylated, linked with cRGD peptide for targeting integrin $\alpha_v\beta_3$ and conjugated with DOTA chelator for ^{64}Cu labeling. It could be demonstrated by *in vitro* competitive binding assay that the nanoconjugate bound specifically to integrin $\alpha_v\beta_3$ in U87MG cells. The radiolabeled nanoparticles were administered in U87MG tumor bearing mice and *in vivo* PET imaging showed integrin specific uptake of the radiotracer, with maximal tumor uptake of ~10 %ID/g at 4 h p.i. These results were further corroborated by T_2-weighted MRI study. Extending this work further, Yang *et al.* further demonstrated the utility of the nanoplatform for targeted anticancer drug delivery and PET/MR imaging.[81] For this purpose, anticancer drug, DOX, was conjugated to the iron oxide nanoparticle in addition to cRGD peptide and NOTA chelator for ^{64}Cu labeling. The radiolabeled and drug loaded iron oxide nanoparticles show good prospects in cancer theranostics.

In an interesting study, Xie *et al.* reported the synthesis of human serum albumin coated iron oxide nanoparticles for multimodality (PET/infrared fluorescence/MR) imaging.[82] The

nanoparticles were conjugated with Cy5.5 dye and DOTA chelator for ^{64}Cu labeling. The nanoplatform was radiolabeled with ^{64}Cu and tested in U87MG tumor bearing mice. *In vivo* PET imaging studies showed rapid and significantly high (~6 %ID/g at 6 h p.i.) tumor uptake with good contrast (Figure 7). The results were further corroborated by near infrared fluorescence and MR imaging (Figure 7),[82] demonstrating the potential of the radiolabeled nanoplatform for multimodality imaging. There are several similar reports from other groups on use of iron oxide nanoparticles for multimodality (PET/near infrared fluorescence/MR/Cerenkov) imaging in preclinical settings.[83–95] For the first time, Chen *et al.* developed a method for chelator free radiolabeling of iron oxide nanoparticle with radio-arsenic ($^{71/72/74/76}$As) ions.[27] The radiolabeled nanoplatform demonstrated good *in vitro* and *in vivo* stability and could be used for dual modality (PET/MR) imaging in mice. As an extension of this work, the same group of authors later reported a method for chelator free radiolabeling of iron oxide nanoparticles with a new relatively new radioisotope, ^{69}Ge.[28] Later Baros *et al.* reported a versatile method for radiolabeling of nanoparticles with different metallic radioisotopes such as ^{64}Cu, ^{89}Zr, ^{111}In, etc.[96] The radiolabeling approach has a wide chemical scope and was found to be applicable to p-, d- and f-block radiometal ions comprising of different ionic sizes and formal oxidation states from +2 to +4. In another attempt to synthesize intrinsically ^{64}Cu-labeled iron oxide nanoparticles, Wong *et al.* developed a rapid, microwave-based synthesis technique to grow dextran-coated iron oxide nanoparticles doped with ^{64}Cu (hydrodynamic diameter ~50 nm) for PET/MR imaging.[97] This facile strategy can also be extended for radiolabeling iron oxide nanoparticles with other radioisotopes and might find wide scale utility in the field of molecular imaging.

Radiolabeled upconversion nanoparticles

Over the last few years, upconversion nanoparticles have received significant interest for their *in vivo* imaging capability as they can emit visual light upon absorption of long wavelength near-infrared photons and demonstrate resistance to photoblinking and photobleaching. [98] In order to develop a multimodality imaging nanoplatform, Zhou *et al.* synthesized ^{18}F-labeled $Gd^{3+}/Yb^{3+}/Er^{3+}$ co-doped $NaYF_4$ nanophosphors that simultaneously possessed radioactivity, magnetic, and up-conversion luminescent properties.[99] The utility of the radiolabeled nanoparticles as multimodal nanoprobe was demonstrated by *in vivo* T_1-weighted MRI and PET imaging in mice model and up-conversion luminescence imaging of living cells and tissue slides. In a similar study, the same group of authors reported a facile technique for ^{18}F-labeling with rare-earth (Y_2O_3, $NaYF_4$, and up-conversion) nanoparticles and demonstrated their utility toward PET/upconversion luminescence imaging.[100]

In another interesting study, Lee *et al.* reported the synthesis of RGD peptide-functionalized Er^{3+}/Yb^{3+} codoped $NaGdF_4$ up-conversion nanoparticles (~30-nm diameter) which could be radiolabeled with ^{124}I for MRI, and PET imaging of tumor angiogenesis in mice bearing glioblastoma (U87MG) xenograft and up-conversion luminescence imaging in U87MG cells.[101] It was observed that the up-conversion luminescence signals from the nanoparticles were specifically localized on the surface of U87MG cells. *In vivo* PET imaging studies showed that the radiolabeled nanoparticles specifically accumulated in U87MG tumors (~2.8 %ID/g at 2 h p.i.), and T_1-weighted MRI showed significant positive contrast

enhancement in U87MG tumors. The tumor localization of the radiolabeled nanoparticles was further confirmed by inductively coupled plasma mass spectrometry and biologic transmission electron microscopy analyses. In a similar study, Gallo *et al.* conjugated DO3A chelator with up-conversion nanoparticles functionalized with RGD peptide and radiolabeled with ^{68}Ga.[102] The radiolabeled nanoparticles could be effectively used for dual modality (PET/up-conversion luminescence) imaging of tumor angiogenesis as in the previous study. Recently, Seo *et al.* reported the synthesis of micelle encapsulated up-conversion nanoparticles conjugated with NOTA chelator for ^{64}Cu labeling.[103] The radiolabeled up-conversion nanoparticles were administered in normal mice. *In vivo* PET imaging and up-conversion luminescence imaging showed the nanoparticles cleared from the biological system primarily through hepatobiliary excretion, which was further verified by TEM investigation. In a recent study, Rieffel *et al.* reported the synthesis of porphyrin phospholipid coated up-conversion nanoparticles (core-shell of $NaYbF_4$:Tm-$NaYF_4$) radiolabeled with ^{64}Cu for hexamodal (up-conversion luminescence, traditional fluorescence, photoacoustic, computed tomography, PET, and Cerenkov luminescence) imaging (Figure 8).[104] In an interesting study, Cui *et al.* reported the synthesis of Fe_3O_4@$NaYF_4$ core/shell nanoparticles with different cation dopants in the shell or core, to form $Co_{0.16}Fe_{2.84}O_4$@$NaYF_4$(Yb, Er) and Fe_3O_4@$NaYF_4$(Yb, Tm) nanoparticles.[105] The synthesized nanoparticles were PEGylated and radiolabeled with ^{18}F/^{64}Cu/^{99m}Tc for triple modality (MRI, PET/SPECT and optical) imaging of sentinel lymph nodes in mice. *In vivo* PET/MR imaging after administration of the radiolabeled nanoparticles in mouse showed that negatively charged $Co_{0.16}Fe_{2.84}O_4$@$NaYF_4$(Yb, Er)-PEG nanoparticles cleared from the blood pool more slowly than positively charged nanoparticles Fe_3O_4@$NaYF_4$(Yb, Tm)-PEG. These studies demonstrated the potential of upconversion nanoparticles as multimodality imaging agents which might find utility toward development of hyperintegrated imaging systems.

Radiolabeled metal sulfide nanoparticles

In recent times, there has been a significant interest toward use of CuS nanoparticles for photothermal ablation therapy of various types of cancers.[24] Compared with other photothermal agents such as gold nanoparticles, CuS nanoparticles offer two major advantages in terms of their translational applications: 1) consistent near infrared absorption; and 2) low cost.[24] When radiolabeled with ^{64}Cu, CuS nanoparticles hold tremendous prospects in cancer theranostics.[24] For the first time, Zhou *et al.* reported the synthesis of intrinsically radiolabeled ^{64}CuS nanoparticles for PET imaging and photothermal therapy of cancer.[106] The CuS nanoparticles were synthesized by metathesis reaction of radioactive $^{64}CuCl_2$, $CuCl_2$ and Na_2S. Well dispersed ^{64}CuS nanoparticles thus formed were then PEGylated to form ^{64}CuS-PEG nanoparticles of ~30-nm hydrodynamic diameter. The PEGylated and non-PEGylated ^{64}CuS nanoparticles were then intravenously administered in mice bearing human glioblastoma (U87MG) tumor xenograft. As expected, the *in vivo* PET imaging and biodistribution studies revealed that tumor uptake was almost 3 times as high with ^{64}CuS-PEG nanoparticles (7.6±1.4 %ID/g) than with non-PEGylated ^{64}CuS nanoparticles (2.6±0.4 %ID/g). Also, the uptake of PEGylated nanoparticles in liver and spleen was much lower than the non-PEGylated nanoparticles. The nanoparticles were also used for photothermal ablation therapy of U87MG tumors in mice model.

This work was further extended by the same group of authors to establish the suitability of intrinsically radiolabeled ^{64}CuS nanoparticles as a theranostic agent in different tumor models [107–109] and for sentinel lymph node mapping.[110] Also, folic acid conjugated ^{64}CuS-PEG nanoparticles were synthesized by the same group for PET imaging and photothermal ablation therapy of folate receptor positive tumors.[111] In an interesting study, the same group has reported the synthesis of CuS nanodots having hydrodynamic diameter of <6 nm, which could efficiently absorb near-infrared light for photothermal ablation therapy, and also stably incorporate ^{64}Cu for PET imaging.[112] The radiolabeled nanodots demonstrated rapid clearance through renalurinary excretion with minimal retention in liver and spleen. Such approaches have the potential to overcome the toxicity issues due to non-specific accumulation of nanoparticles in healthy organs after systemic administration. The utility of reactor produced low specific activity ^{64}Cu toward preparation of intrinsically radiolabeled ^{64}CuS nanoparticles was first demonstrated by Chakravarty *et al.*[32] The biodistribution of the radiolabeled nanoparticles was studied in melanoma tumor bearing mice and the results were comparable to that reported earlier when cyclotron produced “no-carrieradded” grade ^{64}Cu was used for synthesis of the intrinsically radiolabeled nanoparticles. This study opened a new avenue for utilization of low specific activity radioisotopes with excellent nuclear decay characteristics, which otherwise cannot be used for preparation of conventional radiopharmaceuticals.

Inspired by the biomineralization process,[113] CuS nanoparticles have been successfully synthesized in the recent times using natural biopolymers as template. Recently, Wang *et al.* have synthesized ultrasmall CuS nanoparticles inside the cavity of ferritin nanocages by a biomimetic synthesis method.[114] Uniformly sized CuS showed good stability, high water dispersibility, good biocompatibility, strong near infrared absorbance and high photothermal conversion efficiency. The nanoparticles could be efficiently radiolabeled with ^{64}Cu and used for multimodality imaging (photoacoustic/PET imaging) and photothermal ablation therapy in mice bearing U87MG tumor xenograft (Figure 9). This concept of biomineralization-inspired synthesis of CuS nanoplatform for multimodality image-guided cancer theranostics has excellent potential for making clinically translatable advances in foreseeable future.

Other radiolabeled inorganic nanoparticles

Besides the widely used inorganic nanoplatforms described above, there are some other nanoplatforms which have been recently used for radiolabeling with positron emitting radioisotopes. Most of these nanoplatforms comprise of multicomponent nanoparticles, *i.e.*, having at least two different nanoparticles within one structure. Such nanostructures offer synergistic advantages due to each component and hold significant potential in the field of cancer theranostics. Xie *et al.* reported the synthesis of a nanoparticle that is comprised of 8–10-nm gold shell around a 110–120-nm silica sphere.[49] The nanoplatform was conjugated with DOTA chelator for ^{64}Cu labeling and could be used for dual modality (PET/CT) imaging in nude rats bearing head and neck squamous cell carcinoma (HNSCC) xenograft. In another study, Yang *et al.* reported the synthesis of a monodispersed dumbbell shape nanoplatform comprising of two different functional nanomaterials (Au nanoparticles and iron oxide nanoparticles) within one structure.[115] The nanoplatform was conjugated with an

antiepidermal growth factor receptor (anti-EGFR) affibody protein and NOTA chelator. The nanoplatform was radiolabeled with ^{64}Cu and used for dual modality (PET/MR) imaging in A431 tumor bearing mice. In an interesting study, Cui *et al.* reported the synthesis of aluminum hydroxide stabilized magnetic ($MnFe_2O_4$ and Fe_3O_4) nanoparticles, which showed high affinity towards [^{18}F]-fluoride and bisphosphonate groups.[116] Achelator free radiolabeling method was developed by incubating the nanoparticles with [^{18}F]-fluoride or ^{64}Cu-bisphosphonate conjugate with high (>97%) radiolabeling efficiency. The radiolabeled nanoplatforms are potential candidates for use as dual modality contrasts agent for MRI and PET imaging. In a similar study, the utility of chelator free radiolabeling approach was demonstrated by Shi *et al.* using Mg^2Al-layered double hydroxide nanoparticles.[117] The nanoplatform could easily be radiolabeled with bivalent $^{64}Cu^{2+}$ and trivalent $^{44}Sc^{3+}$ cations and used for *in vivo* PET imaging in 4T1 tumor bearing mice.

A new type of nanoplatform comprising of intrinsically radiolabeled ^{64}CuS nanoparticle core with mesoporous silica nanoshells (CuS@MSN) was developed by Chen *et al.*[118] The nanoplatform was conjugated with TRC105 antibody and used for PET imaging of tumor angiogenesis and photoablation therapy in 4T1 tumor bearing mice. In another study from the same group, intrinsically ^{89}Zr labeled PEGylated Gd_2O_2S:Eu nanophosphors were developed for *in vivo* PET/radioluminescence lymph node mapping in mice.[119] Kandanapitiye *et al.* developed a method for incorporation of ^{68}Ga into the crystal structure of Prussian blue to form $K^{68}Ga_xFe_{1-x}$[Fe (CN)$_6$] nanoparticles.[120] This approach is based on the similarity between the Ga^{3+} ion and the Fe^{3+} ion which allowed for partial replacement of Fe^{3+} with Ga^{3+} ions in the crystal structure. This intrinsically radiolabeled nanoplatform could be used as dual modality (PET/MR) imaging agent in preclinical settings.

Recently, Xu *et al.* reported the synthesis of double-PEGylated biocompatible reduced graphene oxide nanosheets anchored with iron oxide nanoparticles.[121] The nanoplatform was conjugated with NOTA chelator and radiolabeled with ^{64}Cu. PET imaging studies were performed in 4T1 tumor bearing mice after administration of the radiolabeled nanoplatform. The radiolabeled nanoplatform exhibited a prolonged blood circulation half-life (~27.7 h) and high tumor uptake (~11 %ID/g). The results of the PET imaging studies could be further corroborated by MRI and photoacoustic imaging studies, demonstrating the potential of the nanoplatform as a multimodality imaging agent (Figure 10).[121] The same group further evaluated the passive targeting capabilities of this long circulating nanoplatform in a murine model of hindlimb ischemia by PET and photoacoustic imaging studies.[122, 123] The authors demonstrated that the radiolabeled nanoplatform passively accumulated in ischemic tissue due to EPR effect, which is decreased as the perfusion normalizes. The results of these studies might be useful for clinical imaging and treatment of peripheral arterial diseases in future.

Clinical studies with radiolabeled inorganic nanoparticles

The first-in-human clinical study of radiolabeled nanoparticles was done with ultrasmall inorganic hybrid nanoparticles known as “C-dots” (Cornell dots).[124] C-dots are inherently fluorescent silica nanoparticles (containing Cy5 dye), modified with PEG and functionalized

with the peptide cyclo-(Arg-Gly-Asp-Tyr) (cRGDY).[124] These 6–7 nm sized particles were radiolabeled with ^{124}I to form ^{124}I-cRGDY–PEG–C dots for dual modality PET/optical imaging. ^{124}I-cRGDY–PEG–C dots demonstrated characteristics of an ideal diagnostic probe in animal models, selectively targeting disease (and metastases) while exhibiting bulk renal clearance. Based on the results of the successful preclinical studies, the radiolabeled nanoparticles received United States Food and Drug Administration (US FDA) approval for use as Investigational New Drug (IND) for targeted molecular imaging of integrin-expressing cancers in human patients.[124, 125] Prior to using these nanoparticles as cancer-targeted optical probes for intraoperative applications, a pilot-scale clinical trial was conducted to evaluate the safety, pharmacokinetics, clearance properties, and radiation dosimetry of a single-injection nanoparticle tracer dose (~185 MBq) in 5 cancer patients with metastatic melanoma using PET imaging.[124] Additionally, metabolic profiles and pathological tests of blood and urine specimens, obtained before and after ^{124}I-cRGDY–PEG–C dots injection, were monitored over a 2-week period. The results of this study indicated that the single dose of the radiotracer was well tolerated in all the 5 patients. The radiolabeled nanoparticles demonstrated appreciably high *in vivo* stability and reproducible pharmacokinetic signatures defined by renal excretion. Preferential uptake and localization (SUV_{max} of the lesion=46.5 at 72 h p.i.) of ^{124}I-cRGDY–PEG–C dots at disease sites were observed in PET imaging (Figure 11). No toxicity related issues or adverse events attributable to the radiolabeled nanoparticles were observed in this limited clinical trial. The overall results of this preliminary clinical trial suggest safe use of ^{124}IcRGDY–PEG–C dots in human cancer diagnostics. However, more rigorous studies in larger population of patients would be required to establish the clinical efficacy of the radiolabeled nanoparticles for PET imaging of human cancers. Nevertheless, this preliminary study has set the stage for widespread clinical utilization of radiolabeled inorganic nanoparticles for PET imaging, which promises to be an important attribute towards improving cancer patient care.

Challenges toward clinical translation of radiolabeled inorganic nanoparticles

Over the last decade, several radiolabeled inorganic nanoparticles have been proposed for PET imaging of cancer in preclinical settings.[13] Despite extensive research efforts from all over the world, except for silica nanoparticles (Cornell dots),[124] radiolabeled inorganic nanoparticles have been hardly incorporated in actual clinical practice thus far. This is particularly because of the difficulties in achieving acceptable pharmacokinetic properties, reproducible nanoparticle uniformity as well as concerns about radiochemical stability, toxicity, biodegradation, and elimination. Additionally, there are some technological and regulatory issues that hinder clinical translation of radiolabeled nanoparticles. In this section, we have discussed the key challenges the radiolabeled nanoparticle formulations face and how these challenges poses unique issues from a clinical or translational point of view.

Biological challenges

The biodistribution of radiolabeled nanoparticles generally tend to be confined to the compartment to which they are administered. If administered locally, they tend to stay around at the site of injection and are then slowly cleared via lymphatic drainage. However,

this approach is limited to superficial tumors and therefore has a very limited scope. If given orally, nanoparticles mostly remain within the gastrointestinal tract and are excreted by way of the feces. Tumor targeting behavior is generally low when radiolabeled nanoparticles are administered by this route and is therefore hardly adopted for PET imaging of cancer. The most widely accepted route of administration of radiolabeled nanoparticles is by intravenous injection. After intravenous injection, depending on hydrodynamic diameter, charge and surface characteristics (*e.g.*, "stealth" coating such as PEGylation),[35] the uptake of radiolabeled nanoparticles occurs in the tumors (generally characterized by fenestrated endothelium and increased leakiness of vasculature) and sites of inflammation.[126] The major limitation of this approach is its inability to reach high tumor-to-background ratio due to non-specific uptake of radiolabeled nanoparticles in healthy organs, such as liver and spleen.

Basically, the mononuclear phagocyte system (MPS), which consists of a system of phagocytic cells, mainly residing in the macrophages in the liver, spleen, and lymph nodes, sequesters nanoparticles immediately after injection.[126] This phenomenon results in high and rapid uptake in these organs. This process of sequestration begins with opsonization of nanoparticles, involving the adsorption of plasma proteins on the surface of radiolabeled nanoparticles.[126] The formation of the protein coating around nanoparticles is dependent on several factors, including nanoparticle size, surface charge, hydrophobicity and surface chemistry. After protein adsorption, the radiolabeled nanoparticles undergo specific attachment to receptors on the surface of phagocytes. Subsequently, the radiolabeled nanoparticles are internalized, transported to phagosomes and fused with lysosomes. In addition to increasing uptake by the MPS, opsonization process often affects active-targeting strategies for radiolabeled nanoparticles, as the adhered protein on nanoparticle surface masks targeting ligands, resulting in significant reduction in specificity of nanoparticles. Moreover, high uptake and prolonged retention of the nanoparticles in liver and spleen results in severe toxicity issues in certain inorganic nanoparticles (such as ^{64}CuS nanoparticles) which is a cause of major concern.[126, 127] To circumvent this limitation, PEG is widely for surface modification of nanoparticles due to its reported "stealth" properties and biocompatibility of the PEGylated nanoparticles. [35] It is generally assumed that PEGylation extends circulation times of the nanoparticles and involves a significant reduction in opsonization, because of which enhanced uptake of radiolabeled nanoparticles occurs in the tumors by both passive targeting (EPR effect) as well as by active targeting. However, there are several contradictory reports which have shown minimal, and even negative, effects of PEGylation.[128] These studies have demonstrated that PEGylation actually causes significant reduction in uptake of nanoparticles by target cells, facilitates enhanced serum protein binding and triggers an immune response that aids toward rapid clearance of the nanoparticles from the biological system.[128] Therefore, it is believed that strong reliance of radiolabeled nanoparticles for cancer imaging on PEGylation might be preventing their further progress toward clinical use.

The size, shape and surface charge of the radiolabeled nanoparticles also dictate their biodistribution in the different organs including the lungs, liver, spleen and kidneys (Figure 12). The nanoparticle size affects several biological phenomena with distinct cut-off size limits that include circulation half-lives, extravasation through leaky vasculature and macrophage uptake.[126] Therefore, it is essential to synthesize nanoparticles with precise

dimensions and high monodispersity. As an example, nanoparticles with hydrodynamic diameters <5 nm undergo fast renal clearance upon intravenous administration and therefore exhibit less toxic effects compared to bigger sized nanoparticles.[126] The endothelial layer in the liver is non-continuous and with vascular fenestrations measuring 50–100 nm, thereby leading to non-specific accumulation of larger sized nanoparticles. Additionally, splenic filtration accounts for retention of particles >200 nm, due to the 200–500 nm size range of interendothelial cell slits.[126] Generally, nanoparticles averaging ~100 nm hydrodynamic diameter remain in circulation for a long time. Longer circulation half-life of radiolabeled nanoparticle will increase their tendency to extravasate through fenestrations in tumor vasculature, which range in size from 380–780 nm.[126] The different shapes of the nanoparticle exhibit unique flow characteristics that significantly change the circulation half-life of the radiolabeled nanoparticles, cell membrane interactions and macrophage uptake, thereby influencing biodistribution among different organs (Figure 12).[126] The surface charge of nanoparticles arises from distinct surface chemistries and affects opsonization, circulation half-life and interaction with resident macrophages of organs comprising the MPS (Figure 12).[126] The positively charged nanoparticles are generally more prone to sequestration by macrophages in the lungs, liver and spleen. On the other hand, neutral or slightly negatively charged nanoparticles have longer circulation half-lives and therefore less accumulation occurs in the MPS organs.

Although the EPR effect in tumors has driven the field of nanoparticle-based tumor targeting,[33] this phenomenon has been shown to vary considerably with the extent of tumor vascularity. Also, EPR effect is generally manifested by uptake of the radiolabeled nanoparticles in the tumor vasculature and interstitial fluid pressures may still be unfavorable toward the flow of nanoparticles into sites of interest.[126] It is also pertinent to mention here that though the EPR effect, which has amply been established in small animal models in preclinical studies, similar evidence is lacking for humans in clinical trials.[126, 129] This is one of the major issues toward clinical translation of radiolabeled nanoparticles. Another issue related to differences between human and animal experiments is the optimization of the number of targeting ligands on a nanoparticle.[126] Generally, this number may not correlate between small animals and humans, or even between two humans.[126] Moreover, in most of the preclinical studies the *in vitro* radiochemical stability studies of the radiolabeled nanoparticles are established arbitrarily without considering the real biological solutions containing proper amounts of biological chelators.

Another important issue, which faces inorganic nanoparticles, is determination of their biological fate and long-term biocompatibility. Although innumerable preclinical studies have reported cellular interactions, biodistribution and subsequent clearance of radiolabeled inorganic nanoparticles, these data could not be normalized with respect to experimental conditions.[129] Therefore, the general conclusions from these studies could not be validated even at the preclinical level. There are some recent reports which suggest that the nanoparticle design parameters (*e.g.*, size, shape, charge, and porosity to name a few) also guides their biocompatibility and biodegradability when administered *in vivo*.[126, 129] As a result, these parameters need to be analytically evaluated at the preclinical level, and also at the clinical level wherever appropriate, to obtain fundamental information on biodistribution, toxicity, and biocompatibility of radiolabeled nanoparticles in order to maximize their

chances for clinical success.[129] Additionally, detailed dosimetry studies would be required before administration of clinically relevant doses of the radiolabeled nanoparticles in human subjects for PET imaging of cancer.[129] Since the dosimetry studies are also based on the kinetics of the radiolabeled nanoparticles, detailed kinetic modeling and distribution studies revealing the role of physicochemical and biological features of nanoparticles should be performed.

Technological and regulatory challenges

Methods to address important technological challenges with radiolabeled nanoparticles such as scaled-up synthesis, process optimization, performance predictions, quality control and quality assurance will be essential in order to ensure the clinical success of future radiolabeled nanoparticle formulations. Furthermore, since the radiolabeled nanoparticles are intended for human use, their preparation must adhere to current good manufacturing process (cGMP) compliance to ensure that the quality of the final product meets the acceptance criteria. The US-FDA has approved a set of regulations describing production of molecular imaging agents according to cGMP, outlined in the Code of Federal Regulations. Enforcement of cGMP is intended to preclude patients at risk due to inadequate safety and quality, and to enhance consistency in the application of the regulatory requirements. Any deviation from the approved method of preparation would require considerable validation before patient use. The United States Pharmacopeia (USP) <797> sterile compounding requirements provide enforceable minimum practice and quality standards for compounded sterile preparations of drug products based on current scientific information and best sterile compounding practices.[130, 131]

While ensuring cGMP compliance for synthesis of radiolabeled nanoparticles is an attractive idea, it is a demanding task as it include requirement of well qualified personnel, use of controlled materials and procedures, accessibility of qualified equipment, synthesis and radiolabeling of nanoparticles in designated clean areas, applying validated processes and analytical methods, full documentation of the process, registration of the radiolabeled agent with national/regional health authorities and release of the same for human use by an authorized personnel. Generally, manual procedure for synthesis and radiolabeling of nanoparticles is used in preclinical settings. However, use of this approach for large-scale clinical applications is challenging. Therefore, it is practical to consider the use of automated synthesis modules due to the following advantages: 1) offer robust, repeatable synthesis of the radiolabeled nanoparticles; 2) reduce operator intervention and thus minimize operational errors; 3) ensure radiation safety; 4) facilitate cGMP compliance and also offer complete traceability of the process, which is an aspect of utmost importance due to the extensive regulatory burden; and 5) reduce the risk of bacterial contamination of the radiolabeled agent which is important from the perspective of clinical use. Despite the excellent attributes of automation strategy, it is important to mention that while undertaking automation process, every operating step needs to be meticulously scrutinized and justified for its necessity since each step would have a direct impact on the overall cost of the module. Moreover, automation process is associated with the challenge of reconfiguring the module for new procedures based on new nanoplatforms or new radioisotopes, whilst maintaining full automation and compliance with cGMP regulations. Nonetheless, in order to be effective

in addressing the particular regulatory barriers, automated synthesis modules should be customized to local legislative, regulatory and institutional conditions.

Conclusions

In summary, we have provided an overview of the inorganic nanoparticles radiolabeled with positron emitting radioisotopes for PET imaging of cancer in preclinical and clinical settings. As a highly sensitive molecular imaging modality, PET can aid toward clinical translational of nanomaterials for early stage disease detection, and monitoring of disease progression, regression, and recurrence. With rapid advances in material science and technology, multifunctional nanoparticles are now being synthesized which combine different functionalities in a single stable nanoconstruct. Such advanced nanomaterials are suitable for multimodality imaging and therapy, with synergistic advantages over any single modality alone. Due to wide diversity in the structures of the nanoparticles, different radiolabeling methods have been developed. These methods are based on the specific requirements for a given application or purpose. Essentially, in any radiolabeling method the radioisotopes should be incorporated onto nanoparticles with appreciably high radiochemical stability and with minimal impact on their original biological behavior.

Although great strides have been made in the use of radiolabeled inorganic nanoparticles for PET imaging of cancer in preclinical settings, most of these studies are in ‘proof-of-principle’ stage and more research efforts are needed to translate radiolabeled nanoparticles to the clinical phase in the near future. As such when a new strategy moves forward toward clinical applications, several types of biological, technological and regulatory challenges emerge which need to be surmounted. Besides these scientific issues, several socio-economic and political factors might also impede clinical translation of radiolabeled inorganic nanoplatforms for PET imaging. Also, complicated bureaucratic protocols in some countries, limited potential market initially for novel molecular imaging agents, lobbying by the manufacturers of other approved imaging probes, lack of reimbursement strategies by the insurance companies for new agents, etc. might also affect the process of clinical translation. Despite these initial hurdles, clinical translation of radiolabeled nanoparticles for the benefit of millions of cancer patient all over the world is definitely feasible with increased interdisciplinary collaboration and knowledge exchange among various stakeholders in this field, which include, funding agencies, regulatory authorities, clinicians, and scientists.

Acknowledgments

Funding.—This work is supported, in part, by the Bhabha Atomic Research Centre (XII-N-R&D-004.01), University of Wisconsin - Madison, the National Institutes of Health (NIBIB/NCI 1R01CA169365, P30CA014520), the American Cancer Society (125246-RSG-13-099-01-CCE).

The authors from Bhabha Atomic Research Centre are grateful to Dr. B. S. Tomar, Director, Radiochemistry and Isotope Group, Bhabha Atomic Research Centre for his constant encouragement and support and to their colleague Dr. Sudipta Chakraborty for fruitful discussion which helped in preparing this manuscript.

References

1. Toy R, Bauer L, Hoimes C, Ghaghada KB, Karathanasis E. Targeted nanotechnology for cancer imaging. Adv Drug Deliv Rev. 2014; 76:79–97. [PubMed: 25116445]

2. Goel S, England CG, Chen F, Cai W. Positron emission tomography and nanotechnology: A dynamic duo for cancer theranostics. Adv Drug Deliv Rev. 2016 Aug 9. [Epub ahead of print].
3. Min Y, Caster JM, Eblan MJ, Wang AZ. Clinical translation of nanomedicine. Chem Rev. 2015; 115:11147–90. [PubMed: 26088284]
4. Etheridge ML, Campbell SA, Erdman AG, Haynes CL, Wolf SM, Mccullough J. The big picture on nanomedicine: The state of investigational and approved nanomedicine products. Nanomedicine. 2013; 9:1–14. [PubMed: 22684017]
5. Anselmo AC, Mitragotri S. A review of clinical translation of inorganic nanoparticles. Aaps j. 2015; 17:1041–54. [PubMed: 25956384]
6. Xing Y, Zhao J, Conti PS, Chen K. Radiolabeled nanoparticles for multimodality tumor imaging. Theranostics. 2014; 4:290–306. [PubMed: 24505237]
7. De Barros AB, Tsourkas A, Saboury B, Cardoso VN, Alavi A. Emerging role of radiolabeled nanoparticles as an effective diagnostic technique. EJNMMI Res. 2012; 2:39. [PubMed: 22809406]
8. Chakravarty R, Hong H, Cai W. Image-guided drug delivery with single-photon emission computed tomography: A review of literature. Curr Drug Targets. 2015; 16:592–609. [PubMed: 25182469]
9. Chakravarty R, Hong H, Cai W. Positron emission tomography image-guided drug delivery: Current status and future perspectives. Mol Pharm. 2014; 11:3777–97. [PubMed: 24865108]
10. Thorek DL, Das S, Grimm J. Molecular imaging using nanoparticle quenchers of cerenkov luminescence. Small. 2014; 10:3729–34. [PubMed: 24861843]
11. Du J, Wang Y, Zhang W. Label-free, non-derivatization cret detection platform for 6-mercaptopurine based on the distance-dependent optical properties of gold nanoparticles. Chemistry. 2012; 18:8540–6. [PubMed: 22639371]
12. Srivatsan A, Chen X. Recent advances in nanoparticle-based nuclear imaging of cancers. Adv Cancer Res. 2014; 124:83–129. [PubMed: 25287687]
13. Sun X, Cai W, Chen X. Positron emission tomography imaging using radiolabeled inorganic nanomaterials. Acc Chem Res. 2015; 48:286–94. [PubMed: 25635467]
14. Cai W, Hong H. In a “nutshell”: Intrinsically radio-labeled quantum dots. Am J Nucl Med Mol Imaging. 2012; 2:136–40. [PubMed: 23133808]
15. Ai F, Ferreira CA, Chen F, Cai W. Engineering of radiolabeled iron oxide nanoparticles for dual-modality imaging. Wiley Interdiscip Rev Nanomed Nanobiotechnol. 2016; 8:619–30. [PubMed: 26692551]
16. Bouziotis P, Psimadas D, Tsotakos T, Stamopoulos D, Tsoukalas C. Radiolabeled iron oxide nanoparticles as dual-modality spect/mri and pet/mri agents. Curr Top Med Chem. 2012; 12:2694–702. [PubMed: 23339765]
17. Nahrendorf M, Keliher E, Marinelli B, Waterman P, Feruglio PF, Fexon L, et al. Hybrid pet-optical imaging using targeted probes. Proc Natl Acad Sci USA. 2010; 107:7910–5. [PubMed: 20385821]
18. Ehlerding EB, Chen F, Cai W. Biodegradable and renal clearable inorganic nanoparticles. Adv Sci (Weinh). 2016; 3
19. Ametamey SM, Honer M, Schubiger PA. Molecular imaging with pet. Chem Rev. 2008; 108:1501–16. [PubMed: 18426240]
20. Deng H, Wang H, Li Z. Matching chelators to radiometals for positron emission tomography imaging-guided targeted drug delivery. Curr Drug Targets. 2015; 16:610–24. [PubMed: 26148988]
21. Price EW, Orvig C. Matching chelators to radiometals for radiopharmaceuticals. Chem Soc Rev. 2014; 43:260–90. [PubMed: 24173525]
22. Perez-Campana C, Gomez-Vallejo V, Puigivila M, Martin A, Calvo-Fernandez T, Moya SE, et al. Biodistribution of different sized nanoparticles assessed by positron emission tomography: A general strategy for direct activation of metal oxide particles. ACS Nano. 2013; 7:3498–505. [PubMed: 23473535]
23. Goel S, Chen F, Ehlerding EB, Cai W. Intrinsically radiolabeled nanoparticles: An emerging paradigm. Small. 2014; 10:3825–30. [PubMed: 24978934]
24. Goel S, Chen F, Cai W. Synthesis and biomedical applications of copper sulfide nanoparticles: From sensors to theranostics. Small. 2014; 10:631–45. [PubMed: 24106015]

25. Sun X, Huang X, Yan X, Wang Y, Guo J, Jacobson O, et al. Chelatorfree (64)cu-integrated gold nanomaterials for positron emission tomography imaging guided photothermal cancer therapy. ACS Nano. 2014; 8:8438–46. [PubMed: 25019252]
26. Shaffer TM, Wall MA, Harmsen S, Longo VA, Drain CM, Kircher MF, et al. Silica nanoparticles as substrates for chelator-free labeling of oxophilic radioisotopes. Nano Lett. 2015; 15:864–8. [PubMed: 25559467]
27. Chen F, Ellison PA, Lewis CM, Hong H, Zhang Y, Shi S, et al. Chelator-free synthesis of a dual-modality pet/mri agent. Angew Chem Int Ed Engl. 2013; 52:13319–23. [PubMed: 24166933]
28. Chakravarty R, Valdovinos HF, Chen F, Lewis CM, Ellison PA, Luo H, et al. Intrinsically germanium-69-labeled iron oxide nanoparticles: Synthesis and in-vivo dual-modality pet/mr imaging. Adv Mater. 2014; 26:5119–23. [PubMed: 24944166]
29. Liu Q, Sun Y, Li C, Zhou J, Li C, Yang T, et al. 18f-labeled magnetic-upconversion nanophosphors via rare-earth cation-assisted ligand assembly. ACS Nano. 2011; 5:3146–57. [PubMed: 21384900]
30. Sun X, Huang X, Guo J, Zhu W, Ding Y, Niu G, et al. Self-illuminating 64cu-doped cdse/zns nanocrystals for in vivo tumor imaging. J Am Chem Soc. 2014; 136:1706–9. [PubMed: 24401138]
31. Hassan PA, Rana S, Verma G. Making sense of brownian motion: Colloid characterization by dynamic light scattering. Langmuir. 2015; 31:3–12. [PubMed: 25050712]
32. Chakravarty R, Chakraborty S, Ningthoujam RS, Vimalnath Nair KV, Sharma KS, Ballal A, et al. Industrial-scale synthesis of intrinsically radiolabeled 64cus nanoparticles for use in positron emission tomography (pet) imaging of cancer. Industrial & Engineering Chemistry Research. 2016; 55:12407–19.
33. Bertrand N, Wu J, Xu X, Kamaly N, Farokhzad OC. Cancer nanotechnology: The impact of passive and active targeting in the era of modern cancer biology. Adv Drug Deliv Rev. 2014; 66:2–25. [PubMed: 24270007]
34. Kunjachan S, Pola R, Gremse F, Theek B, Ehling J, Moeckel D, et al. Passive versus active tumor targeting using rgd- and ngr-modified polymeric nanomedicines. Nano Lett. 2014; 14:972–81. [PubMed: 24422585]
35. Jokerst JV, Lobovkina T, Zare RN, Gambhir SS. Nanoparticle pegylation for imaging and therapy. Nanomedicine (Lond). 2011; 6:715–28. [PubMed: 21718180]
36. Biju V, Itoh T, Ishikawa M. Delivering quantum dots to cells: Bioconjugated quantum dots for targeted and nonspecific extracellular and intracellular imaging. Chem Soc Rev. 2010; 39:3031–56. [PubMed: 20508886]
37. Li ZH, Peng J, Chen HL. Bioconjugated quantum dots as fluorescent probes for biomedical imaging. J Nanosci Nanotechnol. 2011; 11:7521–36. [PubMed: 22097457]
38. Volkov Y. Quantum dots in nanomedicine: Recent trends, advances and unresolved issues. Biochem Biophys Res Commun. 2015; 468:419–27. [PubMed: 26168726]
39. Schipper ML, Cheng Z, Lee SW, Bentolila LA, Iyer G, Rao J, et al. Micropet-based biodistribution of quantum dots in living mice. J Nucl Med. 2007; 48:1511–8. [PubMed: 17704240]
40. Schipper ML, Iyer G, Koh AL, Cheng Z, Ebenstein Y, Aharoni A, et al. Particle size, surface coating, and pegylation influence the biodistribution of quantum dots in living mice. Small. 2009; 5:126–34. [PubMed: 19051182]
41. Tu C, Ma X, House A, Kauzlarich SM, Louie AY. Pet imaging and biodistribution of silicon quantum dots in mice. ACS Med Chem Lett. 2011; 2:285–8. [PubMed: 21546997]
42. Cai W, Chen K, Li ZB, Gambhir SS, Chen X. Dual-function probe for pet and near-infrared fluorescence imaging of tumor vasculature. J Nucl Med. 2007; 48:1862–70. [PubMed: 17942800]
43. Hu K, Wang H, Tang G, Huang T, Tang X, Liang X, et al. In vivo cancer dual-targeting and dual-modality imaging with functionalized quantum dots. J Nucl Med. 2015; 56:1278–84. [PubMed: 26112023]
44. Liu H, Ren G, Miao Z, Zhang X, Tang X, Han P, et al. Molecular optical imaging with radioactive probes. PLoS One. 2010; 5:e9470. [PubMed: 20208993]
45. Xu Y, Liu H, Cheng Z. Harnessing the power of radionuclides for optical imaging: Cerenkov luminescence imaging. J Nucl Med. 2011; 52:2009–18. [PubMed: 22080446]

46. Dothager RS, Goiffon RJ, Jackson E, Harpstrite S, Piwnica-Worms D. Cerenkov radiation energy transfer (cret) imaging: A novel method for optical imaging of pet isotopes in biological systems. PLoS One. 2010; 5:e13300. [PubMed: 20949021]
47. Guo W, Sun X, Jacobson O, Yan X, Min K, Srivatsan A, et al. Intrinsically radioactive [64cu]cuins/zns quantum dots for pet and optical imaging: Improved radiochemical stability and controllable cerenkov luminescence. ACS Nano. 2015; 9:488–95. [PubMed: 25549258]
48. Alex S, Tiwari A. Functionalized gold nanoparticles: Synthesis, properties and applications--a review. J Nanosci Nanotechnol. 2015; 15:1869–94. [PubMed: 26413604]
49. Xie H, Wang ZJ, Bao A, Goins B, Phillips WT. In vivo pet imaging and biodistribution of radiolabeled gold nanoshells in rats with tumor xenografts. Int J Pharm. 2010; 395:324–30. [PubMed: 20540999]
50. Guerrero S, Herance JR, Rojas S, Mena JF, Gispert JD, Acosta GA, et al. Synthesis and in vivo evaluation of the biodistribution of a 18f-labeled conjugate gold-nanoparticle-peptide with potential biomedical application. Bioconjug Chem. 2012; 23:399–408. [PubMed: 22284226]
51. Zhu J, Chin J, Wangler C, Wangler B, Lennox RB, Schirrmacher R. Rapid (18)f-labeling and loading of pegylated gold nanoparticles for in vivo applications. Bioconjug Chem. 2014; 25:1143–50. [PubMed: 24807200]
52. Wang Y, Liu Y, Luehmann H, Xia X, Brown P, Jarreau C, et al. Evaluating the pharmacokinetics and in vivo cancer targeting capability of au nanocages by positron emission tomography imaging. ACS Nano. 2012; 6:5880–8. [PubMed: 22690722]
53. Xiao Y, Hong H, Matson VZ, Javadi A, Xu W, Yang Y, et al. Gold nanorods conjugated with doxorubicin and crgd for combined anticancer drug delivery and pet imaging. Theranostics. 2012; 2:757–68. [PubMed: 22916075]
54. Tian M, Lu W, Zhang R, Xiong C, Ensor J, Nazario J, et al. Tumor uptake of hollow gold nanospheres after intravenous and intra-arterial injection: Pet/ct study in a rabbit vx2 liver cancer model. Mol Imaging Biol. 2013; 15:614–24. [PubMed: 23608932]
55. Cheng K, Kothapalli SR, Liu H, Koh AL, Jokerst JV, Jiang H, et al. Construction and validation of nano gold tripods for molecular imaging of living subjects. J Am Chem Soc. 2014; 136:3560–71. [PubMed: 24495038]
56. Frigell J, Garcia I, Gomez-Vallejo V, Llop J, Penades S. 68ga-labeled gold glyconanoparticles for exploring blood-brain barrier permeability: Preparation, biodistribution studies, and improved brain uptake via neuropeptide conjugation. J Am Chem Soc. 2014; 136:449–57. [PubMed: 24320878]
57. Lee SB, Yoon G, Lee SW, Jeong SY, Ahn BC, Lim DK, et al. Combined positron emission tomography and cerenkov luminescence imaging of sentinel lymph nodes using pegylated radionuclide-embedded gold nanoparticles. Small. 2016; 12:4894–901. [PubMed: 27439987]
58. Chen F, Goel S, Hernandez R, Graves SA, Shi S, Nickles RJ, et al. Dynamic positron emission tomography imaging of renal clearable gold nanoparticles. Small. 2016; 12:2775–82. [PubMed: 27062146]
59. Tao Y, Li M, Ren J, Qu X. Metal nanoclusters: Novel probes for diagnostic and therapeutic applications. Chem Soc Rev. 2015; 44:8636–63. [PubMed: 26400655]
60. Hu H, Huang P, Weiss OJ, Yan X, Yue X, Zhang MG, et al. Pet and nir optical imaging using self-illuminating (64)cu-doped chelator-free gold nanoclusters. Biomaterials. 2014; 35:9868–76. [PubMed: 25224367]
61. Gao F, Cai P, Yang W, Xue J, Gao L, Liu R, et al. Ultrasmall [(64)cu] cu nanoclusters for targeting orthotopic lung tumors using accurate positron emission tomography imaging. ACS Nano. 2015; 9:4976–86. [PubMed: 25919205]
62. Zhao Y, Detering L, Sultan D, Cooper ML, You M, Cho S, et al. Gold nanoclusters doped with (64)cu for cxcr4 positron emission tomography imaging of breast cancer and metastasis. ACS Nano. 2016; 10:5959–70. [PubMed: 27159079]
63. Zhao Y, Sultan D, Detering L, Luehmann H, Liu Y. Facile synthesis, pharmacokinetic and systemic clearance evaluation, and positron emission tomography cancer imaging of (6)(4)cu-au alloy nanoclusters. Nanoscale. 2014; 6:13501–9. [PubMed: 25266128]

64. Frellsen AF, Hansen AE, Jolck RI, Kempen PJ, Severin GW, Rasmussen PH, et al. Mouse positron emission tomography study of the biodistribution of gold nanoparticles with different surface coatings using embedded copper-64. ACS Nano. 2016; 10:9887–98. [PubMed: 27754658]

65. Shi S, Chen F, Cai W. Biomedical applications of functionalized hollow mesoporous silica nanoparticles: Focusing on molecular imaging. Nanomedicine (Lond). 2013; 8:2027–39. [PubMed: 24279491]

66. Huang X, Zhang F, Lee S, Swierczewska M, Kiesewetter DO, Lang L, et al. Long-term multimodal imaging of tumor draining sentinel lymph nodes using mesoporous silica-based nanoprobes. Biomaterials. 2012; 33:4370–8. [PubMed: 22425023]

67. Chen F, Hong H, Zhang Y, Valdovinos HF, Shi S, Kwon GS, et al. In vivo tumor targeting and image-guided drug delivery with antibody-conjugated, radiolabeled mesoporous silica nanoparticles. ACS Nano. 2013; 7:9027–39. [PubMed: 24083623]

68. Chen F, Nayak TR, Goel S, Valdovinos HF, Hong H, Theuer CP, et al. In vivo tumor vasculature targeted pet/nirf imaging with trc105(fab)-conjugated, dual-labeled mesoporous silica nanoparticles. Mol Pharm. 2014; 11:4007–14. [PubMed: 24937108]

69. Goel S, Chen F, Hong H, Valdovinos HF, Hernandez R, Shi S, et al. Vegf(1)(2)(1)-conjugated mesoporous silica nanoparticle: A tumor targeted drug delivery system. ACS Appl Mater Interfaces. 2014; 6:21677–85. [PubMed: 25353068]

70. Chen F, Hong H, Shi S, Goel S, Valdovinos HF, Hernandez R, et al. Engineering of hollow mesoporous silica nanoparticles for remarkably enhanced tumor active targeting efficacy. Sci Rep. 2014; 4:5080. [PubMed: 24875656]

71. Chakravarty R, Goel S, Hong H, Chen F, Valdovinos HF, Hernandez R, et al. Hollow mesoporous silica nanoparticles for tumor vasculature targeting and pet image-guided drug delivery. Nanomedicine (Lond). 2015; 10:1233–46. [PubMed: 25955122]

72. Lee SB, Kim HL, Jeong HJ, Lim ST, Sohn MH, Kim DW. Mesoporous silica nanoparticle pretargeting for pet imaging based on a rapid bioorthogonal reaction in a living body. Angew Chem Int Ed Engl. 2013; 52:10549–52. [PubMed: 23956036]

73. Miller L, Winter G, Baur B, Witulla B, Solbach C, Reske S, et al. Synthesis, characterization, and biodistribution of multiple 89zr-labeled pore-expanded mesoporous silica nanoparticles for pet. Nanoscale. 2014; 6:4928–35. [PubMed: 24675844]

74. Chen F, Goel S, Valdovinos HF, Luo H, Hernandez R, Barnhart TE, et al. In vivo integrity and biological fate of chelator-free zirconium-89-labeled mesoporous silica nanoparticles. ACS Nano. 2015; 9:7950–9. [PubMed: 26213260]

75. Shaffer TM, Harmsen S, Khwaja E, Kircher MF, Drain CM, Grimm J. Stable radiolabeling of sulfur-functionalized silica nanoparticles with copper-64. Nano Lett. 2016; 16:5601–4. [PubMed: 27464258]

76. Goel S, Chen F, Luan S, Valdovinos HF, Shi S, Graves SA, et al. Engineering intrinsically zirconium-89 radiolabeled self-destructing mesoporous silica nanostructures for in vivo biodistribution and tumor targeting studies. Adv Sci (Weinh). 2016; 3:1600122. [PubMed: 27980987]

77. Amstad E, Textor M, Reimhult E. Stabilization and functionalization of iron oxide nanoparticles for biomedical applications. Nanoscale. 2011; 3:2819–43. [PubMed: 21629911]

78. Ittrich H, Peldschus K, Raabe N, Kaul M, Adam G. Superparamagnetic iron oxide nanoparticles in biomedicine: Applications and developments in diagnostics and therapy. Rofo. 2013; 185:1149–66. [PubMed: 24008761]

79. Iv M, Telischak N, Feng D, Holdsworth SJ, Yeom KW, Daldrup-Link HE. Clinical applications of iron oxide nanoparticles for magnetic resonance imaging of brain tumors. Nanomedicine (Lond). 2015; 10:993–1018. [PubMed: 25867862]

80. Lee HY, Li Z, Chen K, Hsu AR, Xu C, Xie J, et al. Pet/mri dual-modality tumor imaging using arginine-glycine-aspartic (rgd)-conjugated radiolabeled iron oxide nanoparticles. J Nucl Med. 2008; 49:1371–9. [PubMed: 18632815]

81. Yang X, Hong H, Grailer JJ, Rowland IJ, Javadi A, Hurley SA, et al. Crgd-functionalized, dox-conjugated, and (6)(4)cu-labeled superparamagnetic iron oxide nanoparticles for targeted

anticancer drug delivery and pet/mr imaging. Biomaterials. 2011; 32:4151–60. [PubMed: 21367450]

82. Xie J, Chen K, Huang J, Lee S, Wang J, Gao J, et al. Pet/nirf/mri triple functional iron oxide nanoparticles. Biomaterials. 2010; 31:3016–22. [PubMed: 20092887]
83. Madru R, Tran TA, Axelsson J, Ingvar C, Bibic A, Ståhlberg F, et al. (68)ga-labeled superparamagnetic iron oxide nanoparticles (spions) for multi-modality pet/mr/cherenkov luminescence imaging of sentinel lymph nodes. American Journal of Nuclear Medicine and Molecular Imaging. 2014; 4:60–9.
84. Jarrett BR, Gustafsson B, Kukis DL, Louie AY. Synthesis of 64cu-labeled magnetic nanoparticles for multimodal imaging. Bioconjug Chem. 2008; 19:1496–504. [PubMed: 18578485]
85. Glaus C, Rossin R, Welch MJ, Bao G. In vivo evaluation of (64)cu-labeled magnetic nanoparticles as a dual-modality pet/mr imaging agent. Bioconjug Chem. 2010; 21:715–22. [PubMed: 20353170]
86. Devaraj NK, Keliher EJ, Thurber GM, Nahrendorf M, Weissleder R. 18f labeled nanoparticles for in vivo pet-ct imaging. Bioconjug Chem. 2009; 20:397–401. [PubMed: 19138113]
87. Sharma R, Xu Y, Kim SW, Schueller MJ, Alexoff D, Smith SD, et al. Carbon-11 radiolabeling of iron-oxide nanoparticles for dual-modality pet/mr imaging. Nanoscale. 2013; 5:7476–83. [PubMed: 23832243]
88. Sun Z, Cheng K, Wu F, Liu H, Ma X, Su X, et al. Robust surface coating for a fast, facile fluorine-18 labeling of iron oxide nanoparticles for pet/mr dual-modality imaging. Nanoscale. 2016; 8:19644–53. [PubMed: 27858030]
89. Locatelli E, Gil L, Israel LL, Passoni L, Naddaka M, Pucci A, et al. Biocompatible nanocomposite for pet/mri hybrid imaging. Int J Nanomedicine. 2012; 7:6021–33. [PubMed: 23271907]
90. Thorek DL, Ulmert D, Diop NF, Lupu ME, Doran MG, Huang R, et al. Non-invasive mapping of deep-tissue lymph nodes in live animals using a multimodal pet/mri nanoparticle. Nat Commun. 2014; 5:3097. [PubMed: 24445347]
91. Tu C, Ng TS, Jacobs RE, Louie AY. Multimodality pet/mri agents targeted to activated macrophages. J Biol Inorg Chem. 2014; 19:247–58. [PubMed: 24166283]
92. Kim SM, Chae MK, Yim MS, Jeong IH, Cho J, Lee C, et al. Hybrid pet/mr imaging of tumors using an oleanolic acid-conjugated nanoparticle. Biomaterials. 2013; 34:8114–21. [PubMed: 23932293]
93. Moon SH, Yang BY, Kim YJ, Hong MK, Lee YS, Lee DS, et al. Development of a complementary pet/mr dual-modal imaging probe for targeting prostate-specific membrane antigen (psma). Nanomedicine. 2016; 12:871–9. [PubMed: 26739097]
94. Aryal S, Key J, Stigliano C, Landis MD, Lee DY, Decuzzi P. Positron emitting magnetic nanoconstructs for pet/mr imaging. Small. 2014; 10:2688–96. [PubMed: 24639392]
95. Torres Martin De Rosales R, Tavare R, Paul RL, Jauregui-Osoro M, Protti A, Glaria A, et al. Synthesis of 64cu(ii)-bis(dithiocarbamateb isphosphonate) and its conjugation with superparamagnetic iron oxide nanoparticles: In vivo evaluation as dual-modality pet-mri agent. Angew Chem Int Ed Engl. 2011; 50:5509–13. [PubMed: 21544908]
96. Boros E, Bowen AM, Josephson L, Vasdev N, Holland JP. Chelate-free metal ion binding and heat-induced radiolabeling of iron oxide nanoparticles. Chemical Science. 2015; 6:225–36. [PubMed: 28553472]
97. Wong RM, Gilbert DA, Liu K, Louie AY. Rapid size-controlled synthesis of dextran-coated, 64cu-doped iron oxide nanoparticles. ACS Nano. 2012; 6:3461–7. [PubMed: 22417124]
98. Park YI, Lee KT, Suh YD, Hyeon T. Upconverting nanoparticles: A versatile platform for wide-field two-photon microscopy and multimodal in vivo imaging. Chem Soc Rev. 2015; 44:1302–17. [PubMed: 25042637]
99. Zhou J, Yu M, Sun Y, Zhang X, Zhu X, Wu Z, et al. Fluorine-18-labeled gd3+/yb3+/er3+ co-doped nayf4 nanophosphors for multimodality pet/mr/ucl imaging. Biomaterials. 2011; 32:1148–56. [PubMed: 20965563]
100. Sun Y, Yu M, Liang S, Zhang Y, Li C, Mou T, et al. Fluorine-18 labeled rare-earth nanoparticles for positron emission tomography (pet) imaging of sentinel lymph node. Biomaterials. 2011; 32:2999–3007. [PubMed: 21295345]

101. Lee J, Lee TS, Ryu J, Hong S, Kang M, Im K, et al. Rgd peptideconjugated multimodal nagdf4:Yb3+/er3+ nanophosphors for upconversion luminescence, mr, and pet imaging of tumor angiogenesis. J Nucl Med. 2013; 54:96–103. [PubMed: 23232276]
102. Gallo J, Alam IS, Jin J, Gu YJ, Aboagye EO, Wong WT, et al. Pet imaging with multimodal upconversion nanoparticles. Dalton Trans. 2014; 43:5535–45. [PubMed: 24535647]
103. Seo HJ, Nam SH, Im HJ, Park JY, Lee JY, Yoo B, et al. Rapid hepatobiliary excretion of micelle-encapsulated/radiolabeled upconverting nanoparticles as an integrated form. Sci Rep. 2015; 5:15685. [PubMed: 26494465]
104. Rieffel J, Chen F, Kim J, Chen G, Shao W, Shao S, et al. Hexamodal imaging with porphyrin-phospholipid-coated upconversion nanoparticles. Adv Mater. 2015; 27:1785–90. [PubMed: 25640213]
105. Cui X, Mathe D, Kovacs N, Horvath I, Jauregui-Osoro M, Torres Martin De Rosales R, et al. Synthesis, characterization, and application of core-shell co0.16fe2. 84o4@nayf4(yb, er) and fe3o4@ nayf4(yb, tm) nanoparticle as trimodal (mri, pet/spect, and optical) imaging agents. Bioconjug Chem. 2016; 27:319–28. [PubMed: 26172432]
106. Zhou M, Zhang R, Huang M, Lu W, Song S, Melancon MP, et al. Achelator-free multifunctional [64cu]cus nanoparticle platform for simultaneous micro-pet/ct imaging and photothermal ablation therapy. J Am Chem Soc. 2010; 132:15351–8. [PubMed: 20942456]
107. Zhou M, Chen Y, Adachi M, Wen X, Erwin B, Mawlawi O, et al. Single agent nanoparticle for radiotherapy and radio-photothermal therapy in anaplastic thyroid cancer. Biomaterials. 2015; 57:41–9. [PubMed: 25913249]
108. Zhou M, Zhao J, Tian M, Song S, Zhang R, Gupta S, et al. Radiophotothermal therapy mediated by a single compartment nanoplatform depletes tumor initiating cells and reduces lung metastasis in the orthotopic 4t1 breast tumor model. Nanoscale. 2015; 7:19438–47. [PubMed: 26376843]
109. Zhou M, Melancon M, Stafford RJ, Li J, Nick AM, Tian M, et al. Precision nanomedicine using dual pet and mr temperature imagingguided photothermal therapy. J Nucl Med. 2016; 57:1778–83. [PubMed: 27283932]
110. Liu Q, Zhou M, Li P, Ku G, Huang G, Li C, et al. 64 cus-labeled nanoparticles: A new sentinel-lymph-node-mapping agent for petct and photoacoustic tomography. Contrast Media Mol Imaging. 2016; 11:475–81. [PubMed: 27523742]
111. Zhou M, Song S, Zhao J, Tian M, Li C. Theranostic cus nanoparticles targeting folate receptors for pet image-guided photothermal therapy. J Mater Chem B Mater Biol Med. 2015; 3:8939–48. [PubMed: 27725882]
112. Zhou M, Li J, Liang S, Sood AK, Liang D, Li C. Cus nanodots with ultrahigh efficient renal clearance for positron emission tomography imaging and image-guided photothermal therapy. ACS Nano. 2015; 9:7085–96. [PubMed: 26098195]
113. Huang P, Yang DP, Zhang C, Lin J, He M, Bao L, et al. Protein-directed one-pot synthesis of ag microspheres with good biocompatibility and enhancement of radiation effects on gastric cancer cells. Nanoscale. 2011; 3:3623–6. [PubMed: 21842073]
114. Wang Z, Huang P, Jacobson O, Wang Z, Liu Y, Lin L, et al. Biomineralization-inspired synthesis of copper sulfide-ferritin nanocages as cancer theranostics. ACS Nano. 2016; 10:3453–60. [PubMed: 26871955]
115. Yang M, Cheng K, Qi S, Liu H, Jiang Y, Jiang H, et al. Affibody modified and radiolabeled gold-iron oxide hetero-nanostructures for tumor pet, optical and mr imaging. Biomaterials. 2013; 34:2796–806. [PubMed: 23343632]
116. Cui X, Belo S, Kruger D, Yan Y, De Rosales RT, Jauregui-Osoro M, et al. Aluminium hydroxide stabilised mnfe2o4 and fe3o4 nanoparticles as dual-modality contrasts agent for mri and pet imaging. Biomaterials. 2014; 35:5840–6. [PubMed: 24768194]
117. Shi S, Fliss BC, Gu Z, Zhu Y, Hong H, Valdovinos HF, et al. Chelator-free labeling of layered double hydroxide nanoparticles for in vivo pet imaging. Sci Rep. 2015; 5:16930. [PubMed: 26585551]
118. Chen F, Hong H, Goel S, Graves SA, Orbay H, Ehlerding EB, et al. In vivo tumor vasculature targeting of cus@msn based theranostic nanomedicine. ACS Nano. 2015; 9:3926–34. [PubMed: 25843647]

119. Zhan Y, Ai F, Chen F, Valdovinos HF, Orbay H, Sun H, et al. Intrinsically zirconium-89 labeled gd2 o2 s:Eu nanoprobes for in vivo positron emission tomography and gamma-ray-induced radioluminescence imaging. Small. 2016; 12:2872–6. [PubMed: 27106630]
120. Kandanapitiye MS, Gott MD, Sharits A, Jurisson SS, Woodward PM, Huang SD. Incorporation of gallium-68 into the crystal structure of prussian blue to form k(68)gaxfe1-x[fe(cn)6] nanoparticles: Toward a novel bimodal pet/mri imaging agent. Dalton Trans. 2016; 45:9174–81. [PubMed: 27169624]
121. Xu C, Shi S, Feng L, Chen F, Graves SA, Ehlerding EB, et al. Long circulating reduced graphene oxide-iron oxide nanoparticles for efficient tumor targeting and multimodality imaging. Nanoscale. 2016; 8:12683–92. [PubMed: 27109431]
122. Im HJ, England CG, Feng L, Graves SA, Hernandez R, Nickles RJ, et al. Accelerated blood clearance phenomenon reduces the passive targeting of pegylated nanoparticles in peripheral arterial disease. ACS Appl Mater Interfaces. 2016; 8:17955–63. [PubMed: 27340833]
123. England CG, Im HJ, Feng L, Chen F, Graves SA, Hernandez R, et al. Re-assessing the enhanced permeability and retention effect in peripheral arterial disease using radiolabeled long circulating nanoparticles. Biomaterials. 2016; 100:101–9. [PubMed: 27254470]
124. Phillips E, Penate-Medina O, Zanzonico PB, Carvajal RD, Mohan P, Ye Y, et al. Clinical translation of an ultrasmall inorganic optical-pet imaging nanoparticle probe. Sci Transl Med. 2014; 6:260ra149.
125. Benezra M, Penate-Medina O, Zanzonico PB, Schaer D, Ow H, Burns A, et al. Multimodal silica nanoparticles are effective cancer-targeted probes in a model of human melanoma. J Clin Invest. 2011; 121:2768–80. [PubMed: 21670497]
126. Blanco E, Shen H, Ferrari M. Principles of nanoparticle design for overcoming biological barriers to drug delivery. Nat Biotechnol. 2015; 33:941–51. [PubMed: 26348965]
127. Li J, Chang X, Chen X, Gu Z, Zhao F, Chai Z, et al. Toxicity of inorganic nanomaterials in biomedical imaging. Biotechnol Adv. 2014; 32:727–43. [PubMed: 24389087]
128. Verhoef JJ, Anchordoquy TJ. Questioning the use of pegylation for drug delivery. Drug Deliv Transl Res. 2013; 3:499–503. [PubMed: 24932437]
129. Choi H, Lee Y-S, Hwang Do W, Lee Dong S. Translational radionanomedicine: A clinical perspective. European Journal of Nanomedicine. 2016:71.
130. Dash A, Chakraborty S, Pillai MR, Knapp FF Jr. Peptide receptor radionuclide therapy: An overview. Cancer Biother Radiopharm. 2015; 30:47–71. [PubMed: 25710506]
131. 2012 USP 35 NF 30. USP-NF General Chpater <797> Pharmaceutical compounding -sterile preparations. Available from https://www.snmmi.org/files/docs/USP%20797.pdf [cited 2017, Jan 25]

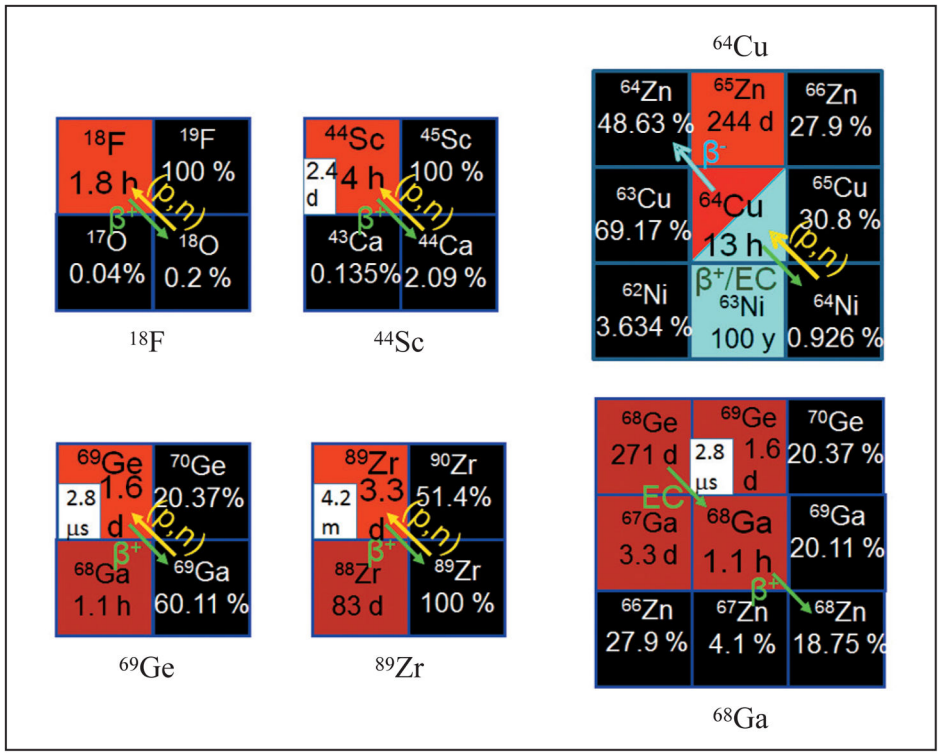

Figure 1.

Schematic representation of the production and nuclear decay of the radioisotopes commonly used for radiolabeling inorganic nanoparticles for PET imaging.

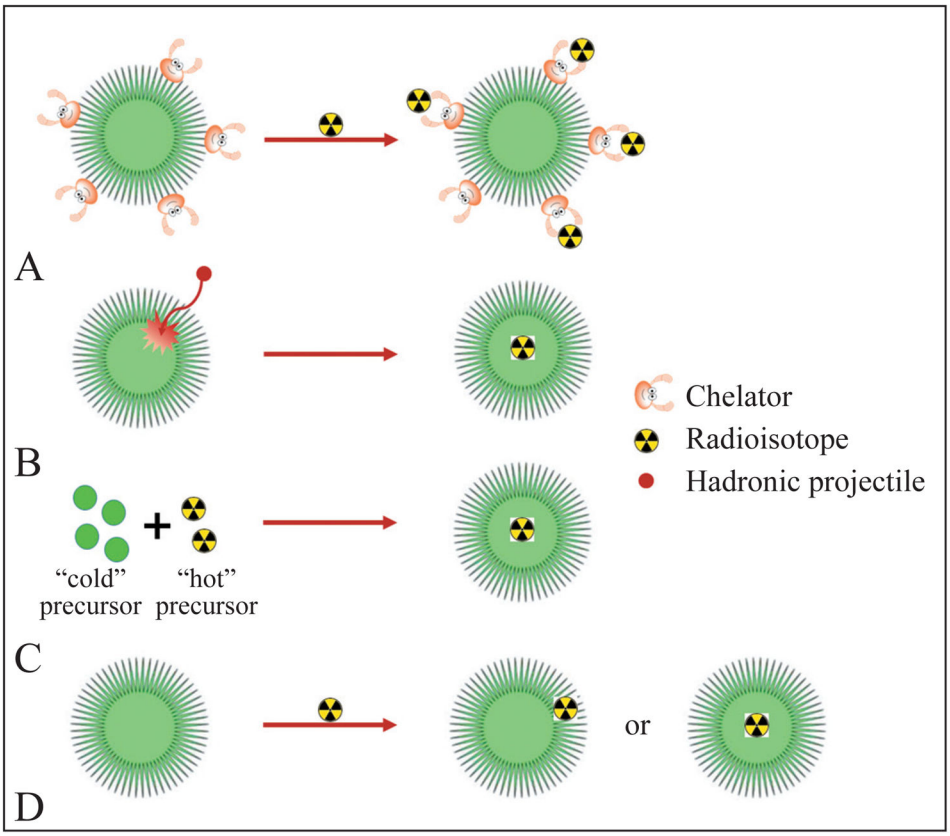

Figure 2.

Schematic representation of the methods for radiolabeling inorganic nanoparticles by (A) coordination of radiometal ions with chelators, (B) direct bombardment of nanoparticles with hadronic projectiles, (C) direct synthesis of nanoparticles using radioactive and non-radioactive precursors, and (D) post-synthesis radiolabeling without using chelator.

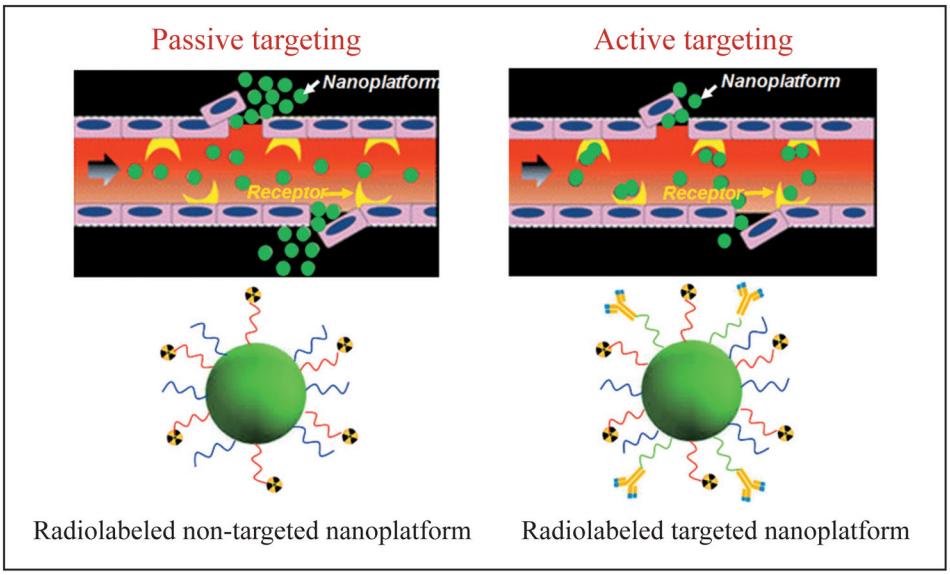

Figure 3.

Schematic representation of EPR mediated passive targeting and active targeting using radiolabeled inorganic nanoparticles. Nanoparticles can passively target tumors through preferential passage through larger interendothelial junctions compared to those of healthy tissues. Nanoparticles can also be conjugated with suitable targeting agents, such as antibodies which are specific to proteins (receptors) more highly expressed in tumors than healthy tissue, to actively target tumors. Adapted from Kunjachan *et al.*[34]

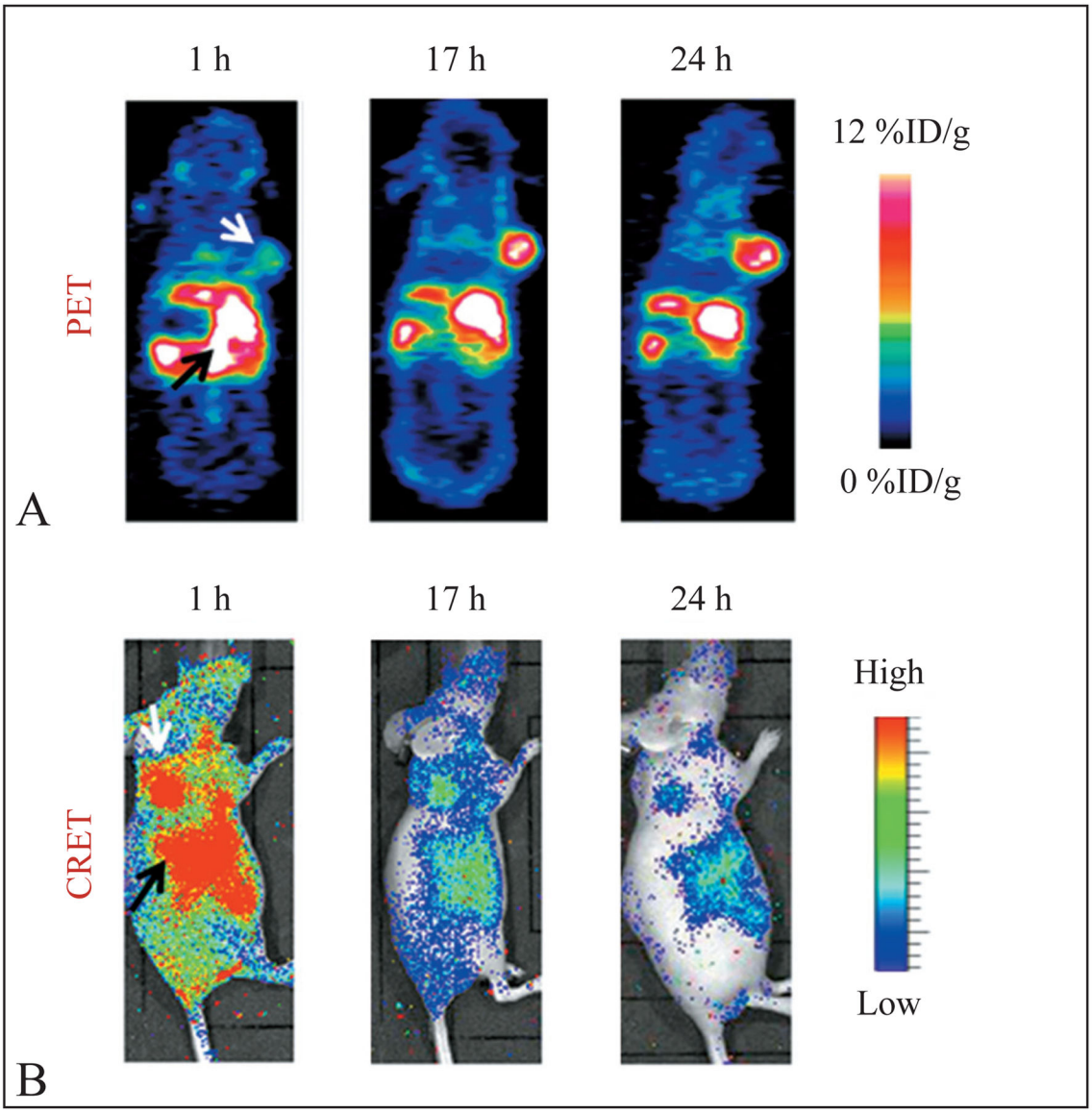

Figure 4.

Molecular imaging using radiolabeled quantum dots. A) Representative whole-body coronal PET images of U87MG tumor-bearing mice at 1, 17, and 24 h p.i. of ^{64}Cu-labeled quantum dots. White arrow indicates tumor area; black arrow indicates liver area. B) Representative whole-body luminescence images of U87MG tumor-bearing mice at 1, 17, and 24 h p.i. of ^{64}Cu-labeled quantum dots. White arrow indicates tumor area; black arrow indicates liver area. Adapted from Sun *et al.*[30]

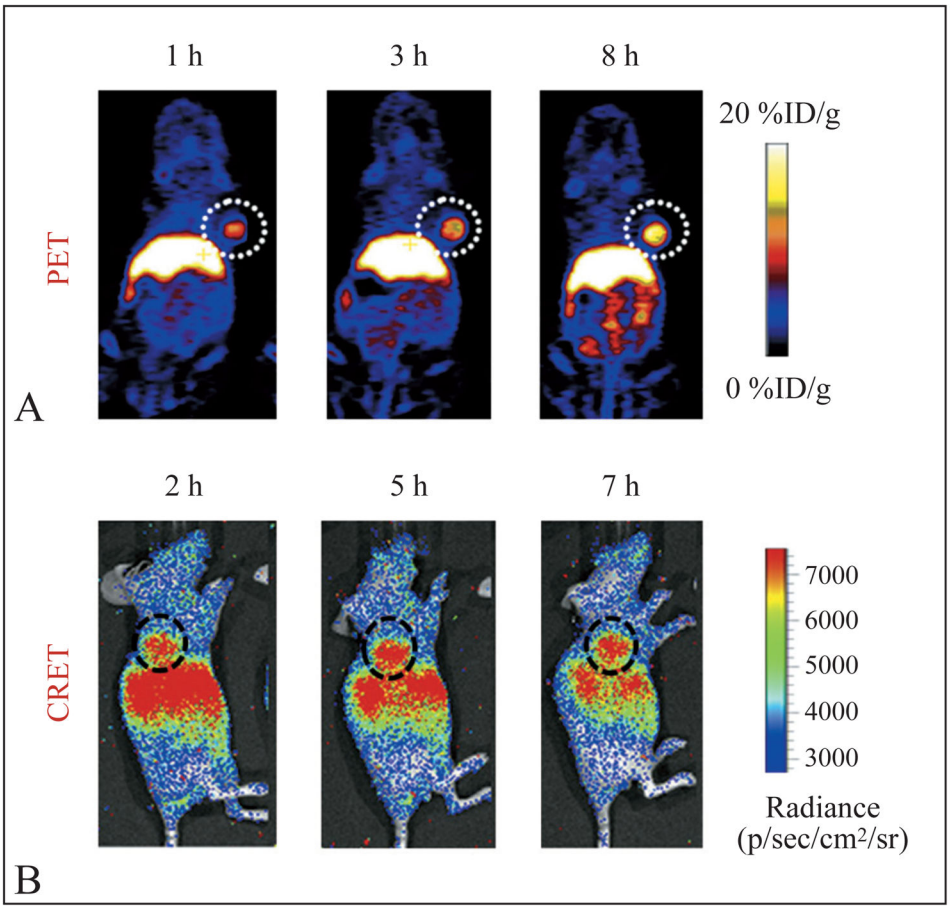

Figure 5.

Molecular imaging using radiolabeled gold nanoclusters. A) Representative PET images of U87MG tumor-bearing mice at 1, 3, and 8 h p.i. of ^{64}Cu-doped gold nanoclusters. Tumor is indicated by white circle; B) representative self-illuminating near infrared images of U87MG tumor-bearing mice at 1, 3, and 8 h p.i. of ^{64}Cu-doped gold nanoclusters. Tumor is indicated by black circle. Adapted from Gao *et al.*[60]

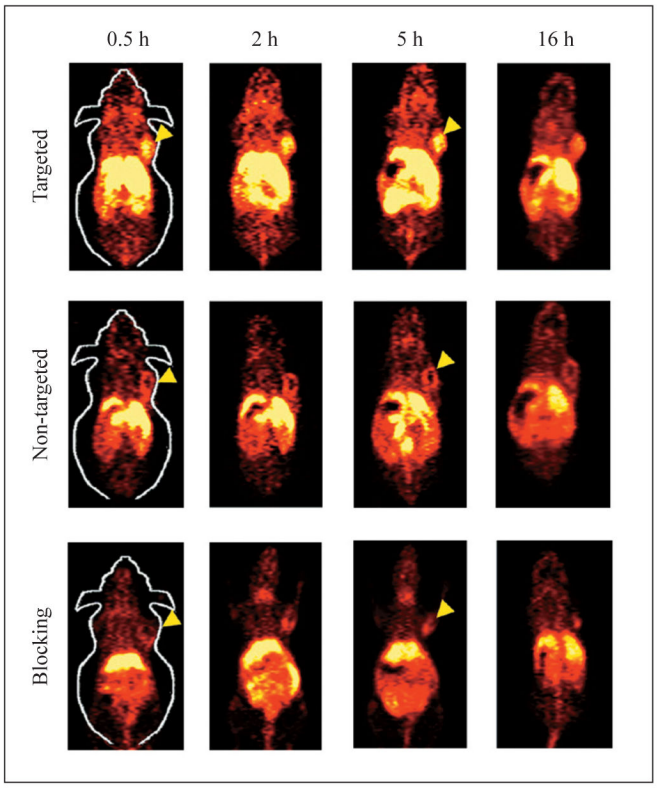

Figure 6.

Molecular imaging using radiolabeled silica nanoparticle. Representative PET images of 4T1 tumor-bearing mice at 0.5, 2, 5, 16 h p.i. of (i) ^{64}Cu-labeled mesoporous silica nanoparticles conjugated with TRC105 (targeted), (ii) ^{64}Cu-labeled mesoporous silica nanoparticles (non-targeted), or (c) ^{64}Cu-labeled mesoporous silica nanoparticles conjugated with TRC105 with a blocking dose of TRC105 (blocking). Tumors were indicated by yellow arrowheads. Adapted from Chen *et al.*[67]

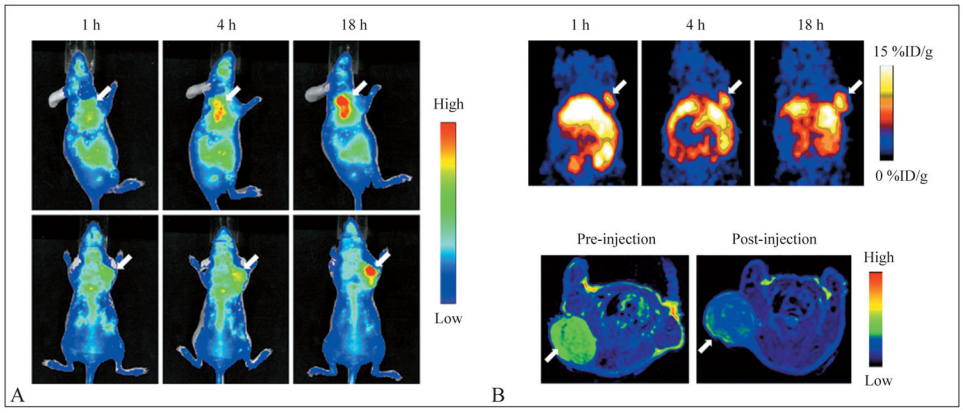

Figure 7.

Molecular imaging using radiolabeled iron oxide nanoparticles. A) Representative *in vivo* near infrared images of U87MG tumor-bearing mice at 1 h, 4 h and 18 h p.i. of ^{64}Cu-labeled iron oxide nanoparticles; B) representative *in vivo* PET images results of U87MG tumor-bearing mice at 1 h, 4 h and 18 h p.i. of ^{64}Cu-labeled iron oxide nanoparticles; C) representative MRI images of U87MG tumor-bearing mice acquired before and 18 h p.i. Adapted from Xie *et al.*[82]

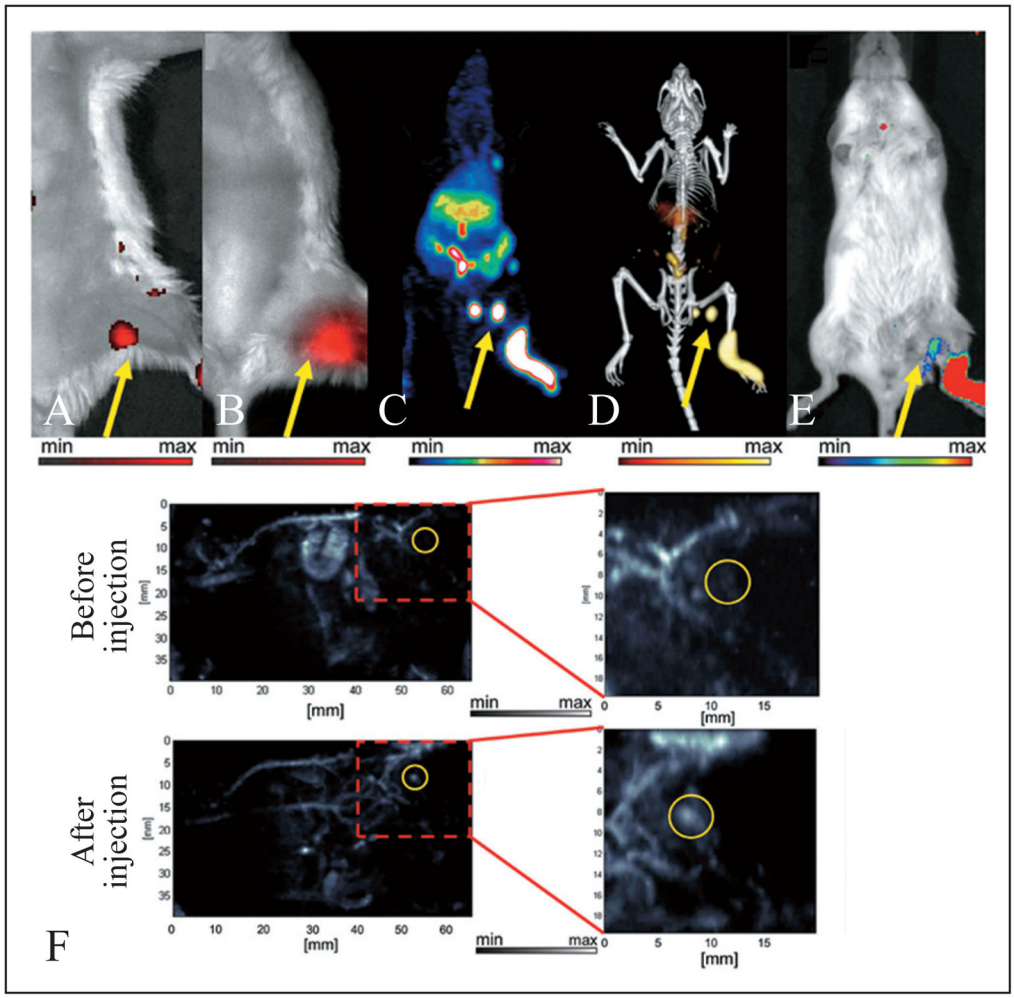

Figure 8.

Molecular imaging using radiolabeled upconversion nanoparticles. The radiolabeled upconversion nanoparticles were injected in the rear left footpad and imaged in six different modalities at 1 h p.i. Accumulation of the nanoparticles in the first draining lymph node is indicated with yellow arrows. A) Traditional fluorescence; B) upconversion image; C) PET image; D) merged PET/CT image; E) chemiluminescence image; F) photoacoustic images before and after injection show endogenous photoacoustic blood signal compared to the contrast enhancement that allowed visualization of the previously undetected lymph node. Adapted from Rieffej *et al.*[104]

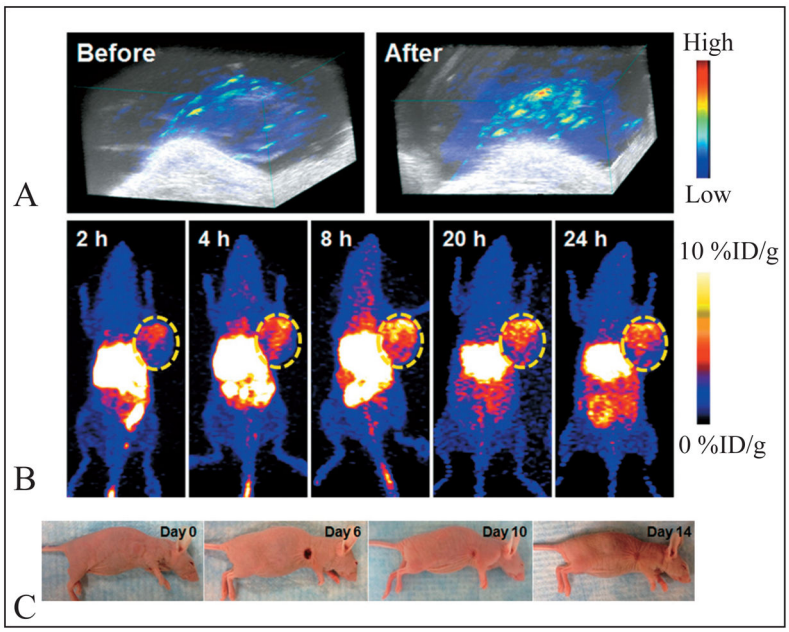

Figure 9.

Molecular imaging and photothermal ablation therapy using intrinsically radiolabeled ^{64}CuS nanoparticles. A) Representative 3D photoacoustic images of U87MG tumor pre- and post-injection of CuS nanoparticles; B) representative *in vivo* PET images results of U87MG tumor-bearing mice at 2, 4, 8, 20, and 24 h p.i. of ^{64}CuS nanoparticles; C) representative photos of U87MG tumor-bearing mice at different days after treatment. Adapted from Wang *et al.*[114]

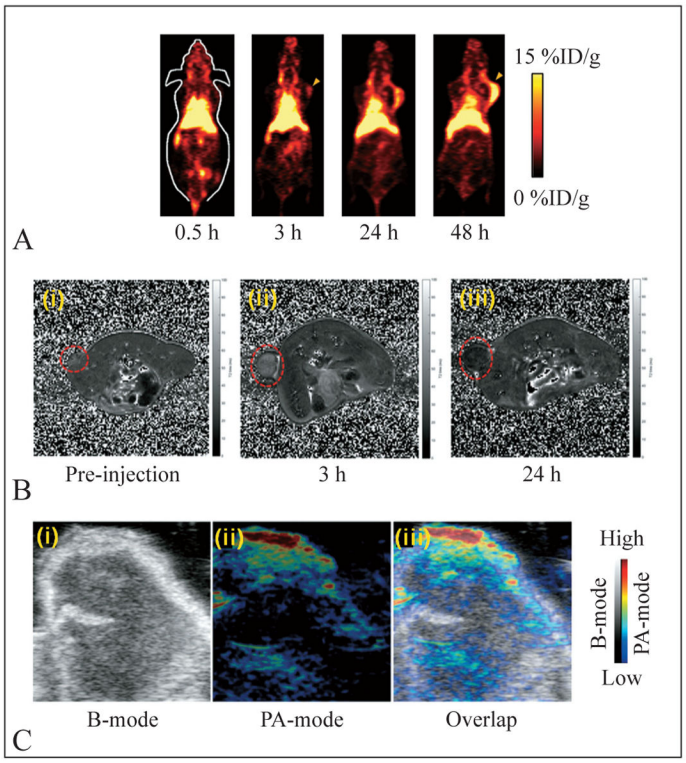

Figure 10.

Molecular imaging using radiolabeled reduced graphene oxide nanosheets anchored with iron oxide nanoparticles. A) Representative *in vivo* PET images results of 4T1 tumor-bearing mice at 0.5 h, 3 h, 24 h and 48 h p.i. of ^{64}Cu-labeled nanoparticles; B) representative MR images acquired before (i) and after 3 h (ii) and 24 h (iii) intravenous injection of nanoparticles in 4T1 tumor-bearing mice; C) representative photoacoustic images of the tumor part in 4T1 tumor-bearing mouse with intravenous injection of nanoparticles. Adapted from Xu *et al.*[121]

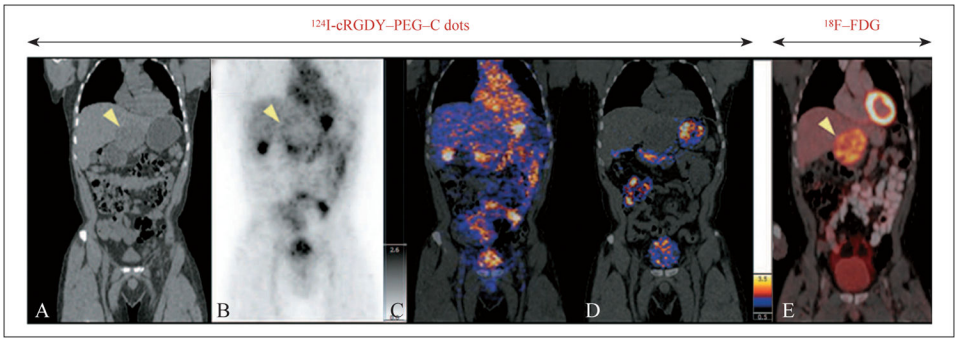

Figure 11.

Clinical PET/CT imaging of nanoparticle biodistribution and tumor uptake after systemic administration of ^{124}I-cRGDY–PEG–C dots. A) Coronal CT in patient shows a hypodense left hepatic lobe metastasis (arrowhead); B) coronal PET image at 4 h p.i. shows radiolabeled nanoparticle activity along the peripheral aspect of the tumor (arrowhead), in addition to the bladder, gastrointestinal tract (stomach, intestines), gallbladder, and heart; C, D) co-registered PET/CT at 4 h (C) and 24 h (D) p.i. localizes activity to the tumor margin; E) corresponding ^{18}F-FDG PET-CT image showing the hepatic metastasis in (A) (arrowhead). The color scale represents SUV values. Adapted from Phillips *et al.*[124]

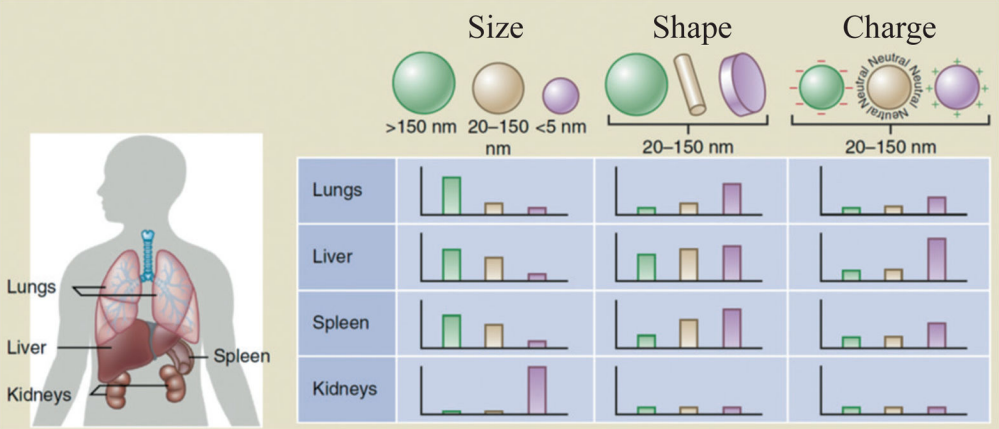

Figure 12.

The size, shape and surface charge of radiolabeled inorganic nanoparticles dictate their biodistribution among different organs including the liver, lungs, spleen and kidneys, which is an important aspect toward their clinical translation. Adapted from Blanco *et al.*[126]

Table I

Nuclear decay characteristics of some positron emitting radioisotopes which can be used for radiolabeling inorganic nanoparticles for use in PET imaging.

Radionuclide	Half-life (h)	Mode of decay	β^+ particle energy (MeV)[#,@]	β^+-branching ratio (%)[@]	Major γ-photons emitted other than annihilation photons in MeV (% abundance)
^{18}F	1.8	β^+/ECD	0.633	97.0	None
^{44}Sc	3.9	β^+/ECD	1.474	94.3	1.157 (99.9)
^{64}Cu	12.7	β^+/β^-/ECD	0.653	17.4	1.346 (0.47)
^{68}Ga	1.1	β^+/ECD	1.889	88.0	1.077 (3.3)
^{69}Ge	39.1	β^+/ECD	1.205	21.0	0.574 (13.3), 0.872 (11.9)
^{72}As	26.0	β^+/ECD	2.499	64.2	0.630 (7.9), 0.834 (80.0),
^{86}Y	14.7	β^+/ECD	1.220	11.9	0.443 (16.9), 0.646 (9.2), 0.777 (22.4), 1.854 (17.4), 1.920 (20.8)
^{89}Zr	78.4	β^+/ECD	0.897	23.0	0.909 (100)

[#]Maximum β^+ energy is mentioned;

[@]Only principal β^+ emission is indicated.

ECD: electron capture decay.

Table II

Representative examples of preclinical studies carried out using radiolabeled inorganic nanoparticles as probes.

Nanoplatform	Size (nm)	Radioisotope used	Molecular imaging modalities used	Targeting ligand	Cancer model	Maximal tumor uptake (%ID/g)	Ref.
Quantum dots	~ 100	^{18}F	PET, near infrared fluorescence	β-Glu-RGD-BBN (RGD is arginine-glycine-aspartate acid, and BBN is bombesin)	Prostate cancer (PC3)	~ 2.5	43
Gold nanoparticles	~ 7	^{64}Cu	PET, photoacoustic	RGD peptide	Glioblastoma (U87MG)	~ 7.9	55
Mesoporous silica nanoparticles	~ 150	^{64}Cu	PET, near infrared fluorescence	TRC105 monoclonal antibody	Murine breast cancer (4T1)	~ 10	70
Iron oxide nanoparticles	~ 68	^{64}Cu	PET, CT	RGD peptide	Glioblastoma (U87MG)	~ 5	81
Upconversion nanoparticles	~ 24	^{124}I	Upconversion luminescence, MRI, and PET	RGD peptide	Glioblastoma (U87MG)	~ 3	101
CuS nanoparticles	~ 30	^{64}Cu	PET, CT	Folic acid	KB tumor cells	~ 10	111
Au-Iron oxide hetero-nanostructures	~ 25	^{64}Cu	PET, near infrared, MRI	anti-EGFR affibody protein	Epidermoid carcinoma (A431)	~ 5	115